ASTRON

Netherlands Institute for Radio Astronomy

RM Synthesis: Application to (Spiral) Galaxies

George Heald, Robert Braun & Rainer Beck

DFG RU 1254 Kickoff, Irsee

4 October 2010

ASTRON is part of the Netherlands Organisation for Scientific Research (NWO)

Overview

- Review of the RM Synthesis technique
- WSRT-SINGS: data & analysis
- Trends in the WSRT-SINGS observations
- Interpretation: global magnetic field geometry in spiral galaxies
- Predictions and future work

- See:
  Brentjens & de Bruyn 2005 (A&A, 441, 1217) [RM Synthesis]
  Braun et al. 2007 (A&A, 461, 455) [WSRT-SINGS survey description]
  Heald et al. 2009 (A&A, 503, 409) [WSRT-SINGS polarization data analysis]
  Braun et al. 2010 (A&A, 514, 42) [Global magnetic field geometries]

Synchrotron radiation

- cosmic ray electrons spiraling around magnetic field lines
- beamed radiation in direction of electron motion
- linearly polarized perpendicular to magnetic field
- continuum radiation with power law index related to power law index of electron energy spectrum

Polarized synchrotron radiation traces $B_{\perp}$

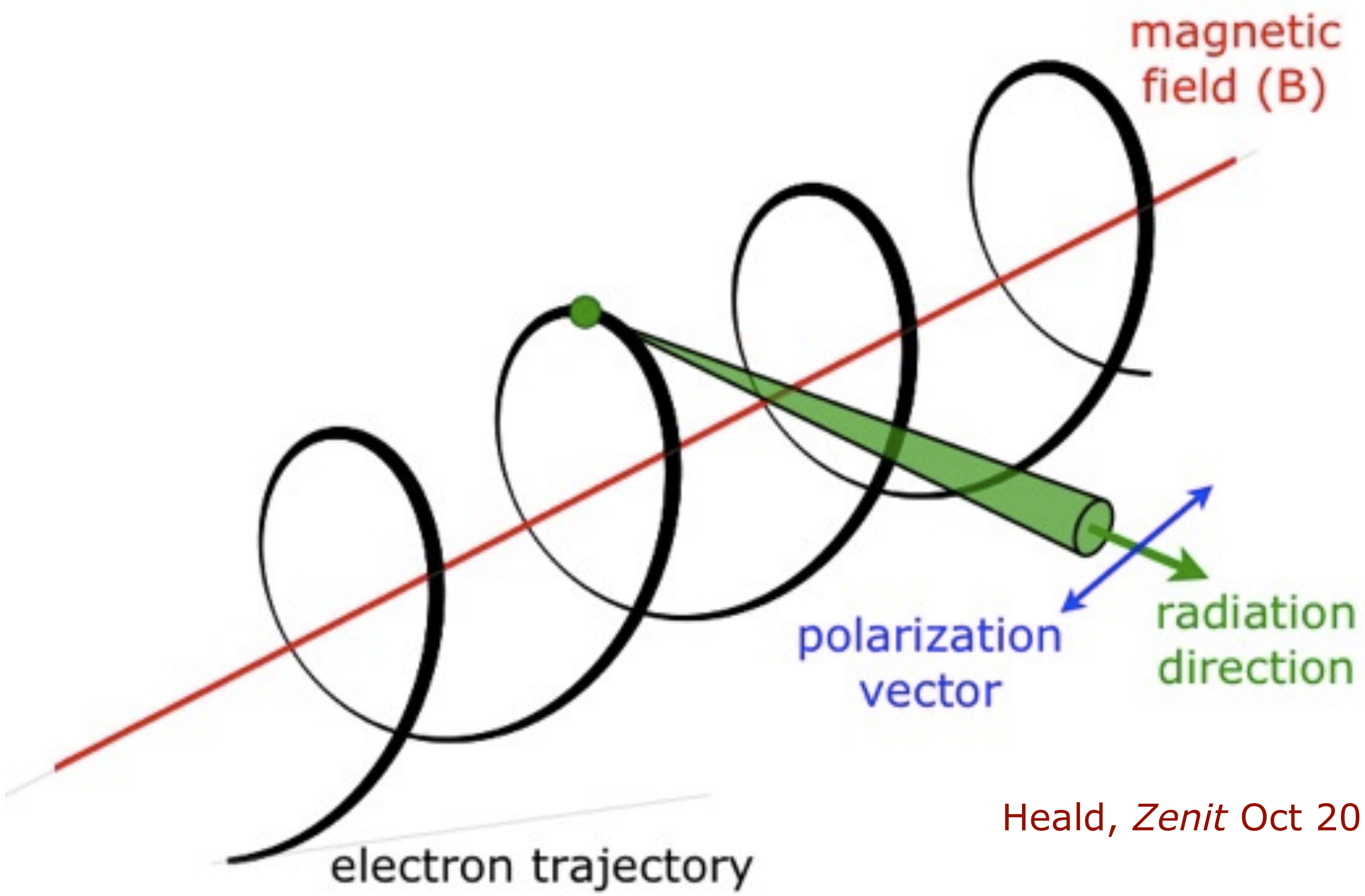

Heald, *Zenit* Oct 2010

Faraday rotation

- Magnetized plasma is birefringent - causes Faraday rotation
- Speed of light different for right and left circular polarization
- Because RL phase difference is determined by
  - difference in c for R,L
  - wavelength of radiation
- and RL phase difference determines the polarization angle, we get a frequency-dependent change in linear polarization angle

Faraday rotation traces $B_{||}$

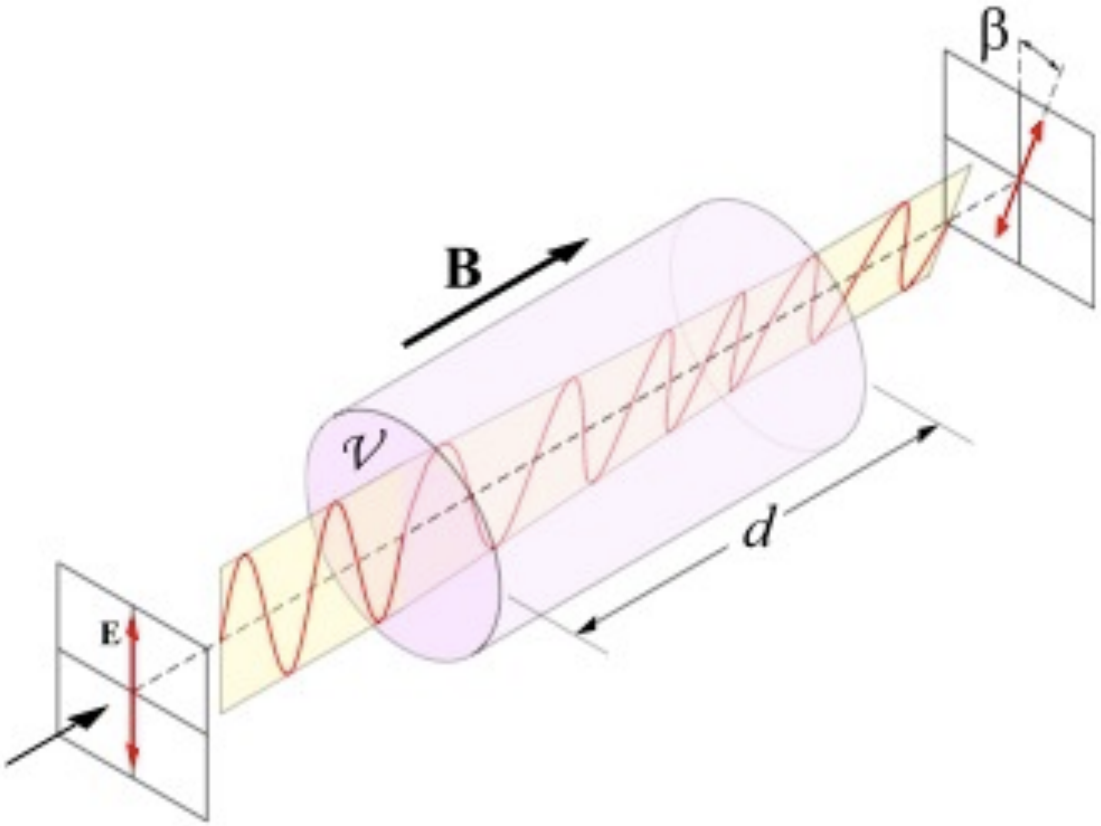

Faraday depth

- Not directly related to physical depth!

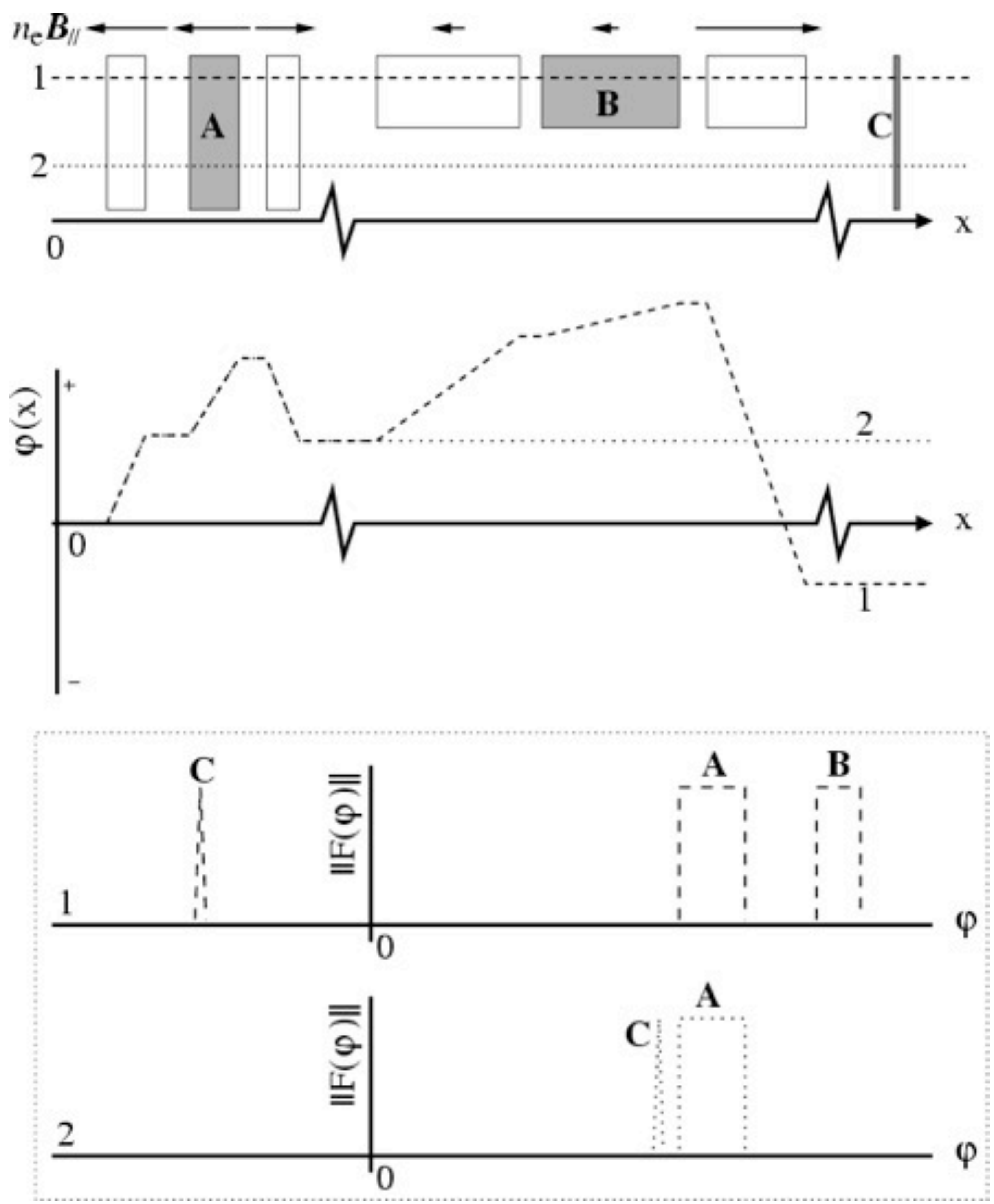

Brentjens & de Bruyn (2005)

Depolarization mechanisms

- Depth depolarization / turbulent depolarization
- Beam depolarization
- Bandwidth depolarization

Faraday Rotation

- Faraday rotation caused by LOS magnetic field, and thermal electrons:

$$\mathrm{RM} \propto \int n_e \, \vec{B} \cdot d\vec{l}$$

- It is frequency dependent:

$$\chi = \chi_0 + \mathrm{RM} \times \lambda^2$$

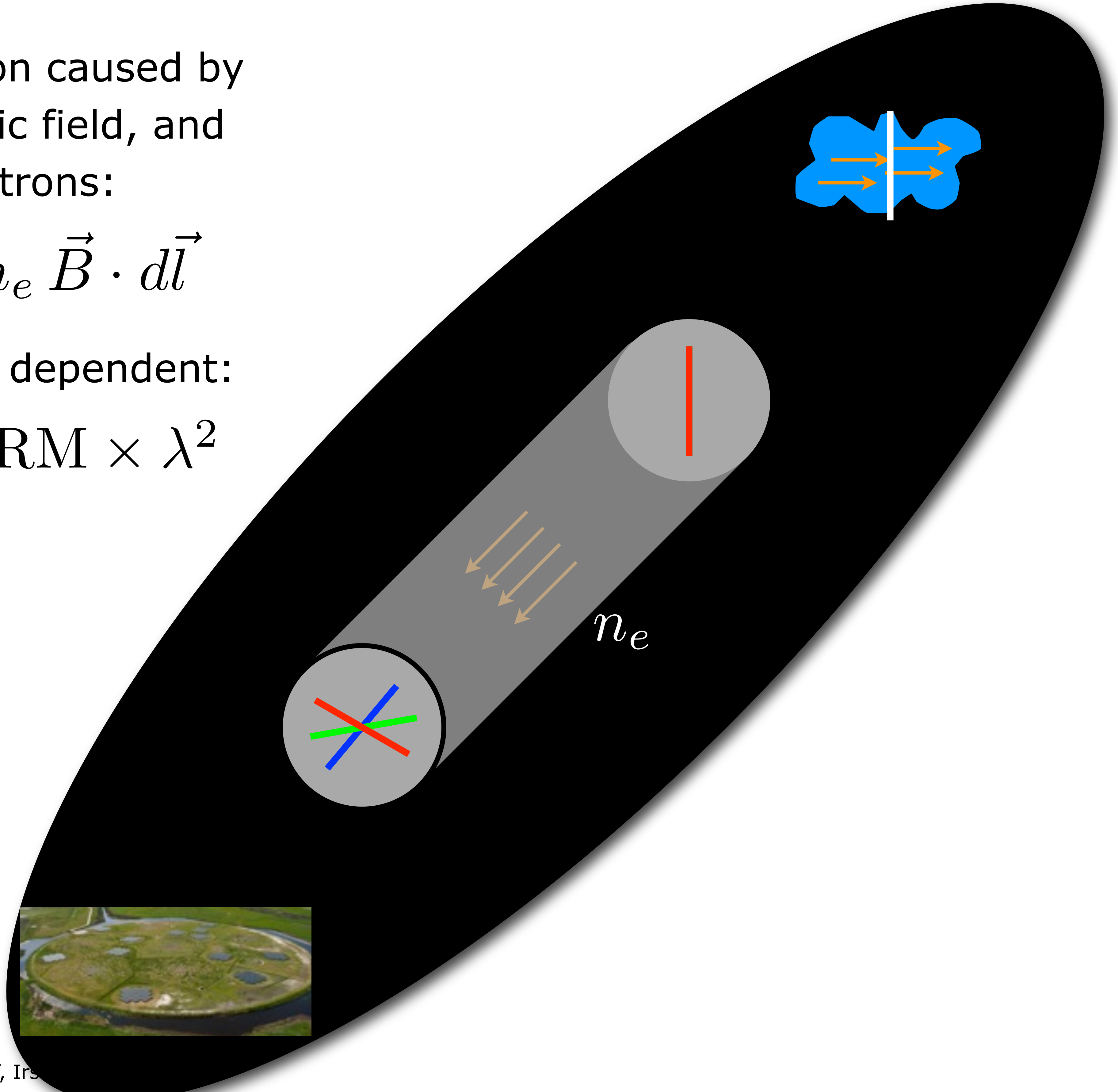

- The nπ ambiguity

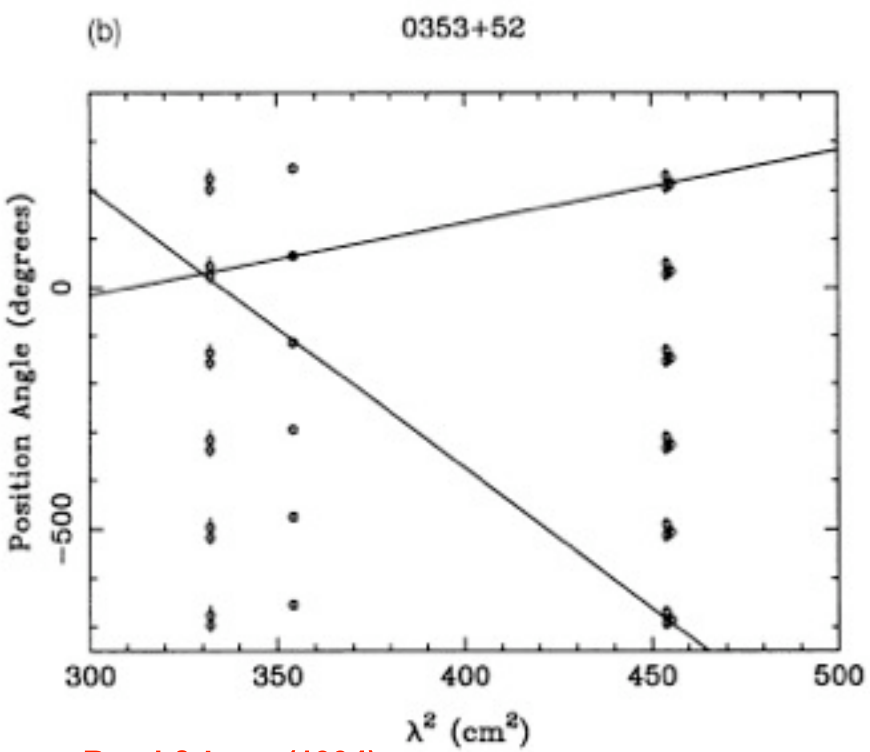

Rand & Lyne (1994)

RM synthesis was developed to combat this problem.

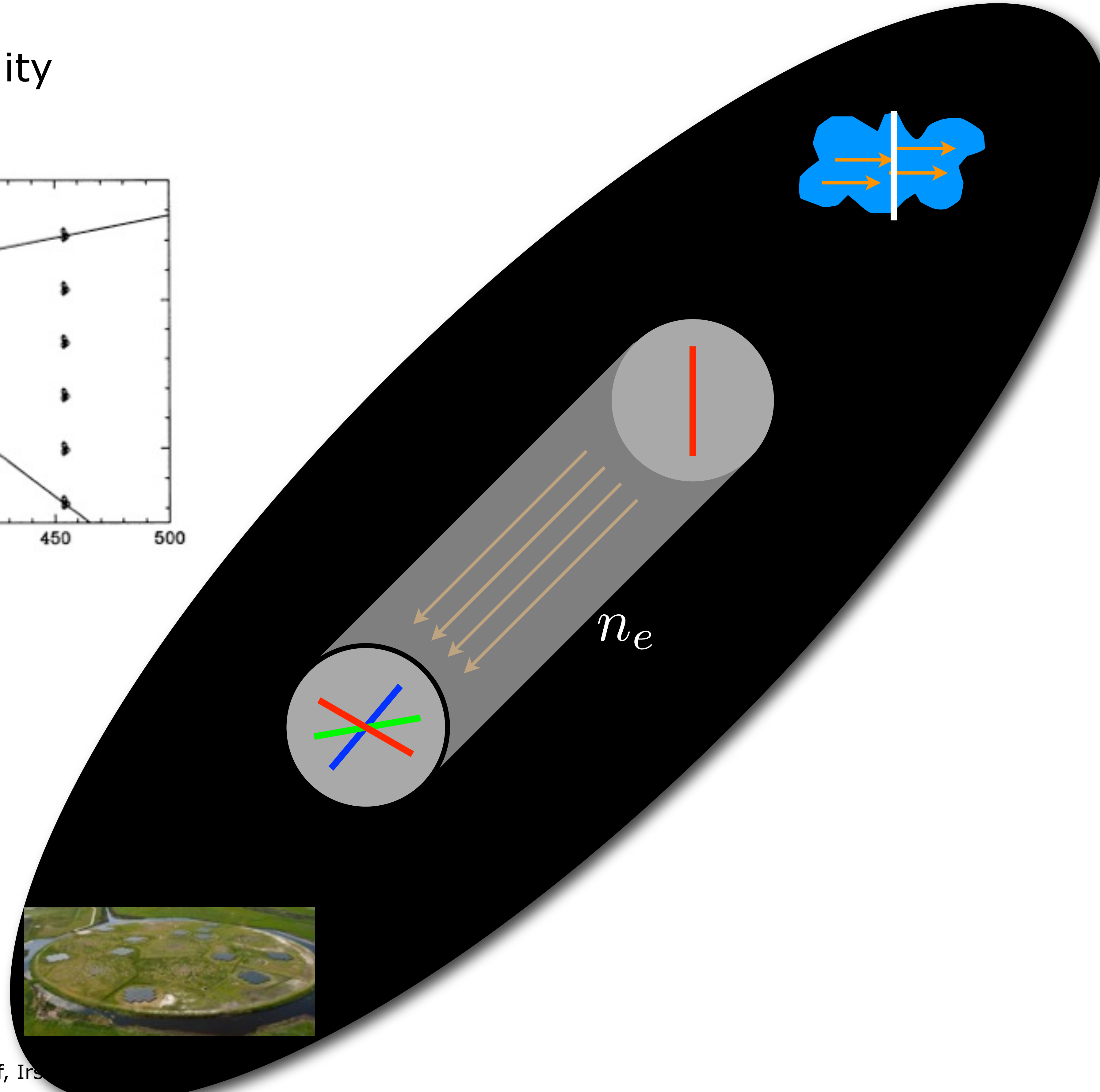

RM Synthesis: In theory

- Polarization vector:

$$\vec{P} = p\,I\,e^{2i\chi}$$

but since

$$\chi \;=\; \mathrm{RM} \times \lambda^2$$

and redefining

$$\phi \equiv \mathrm{RM}$$

where ϕ is the "Faraday depth", we can write a more general expression

$$P(\lambda^2) = \int_{-\infty}^{+\infty} F(\phi) e^{2i\phi\lambda^2} d\phi$$

(Burn 1966)

RM Synthesis: In theory

- Generic form of the expression for rotation measure is (Burn 1966):

$$P(\lambda^2) = \int_{-\infty}^{+\infty} F(\phi) e^{2i\phi\lambda^2} d\phi$$

  where ϕ (the ***Faraday depth***) has taken the place of RM, and F is the ***Faraday dispersion function***.

- Faraday dispersion function of a Burn slab is a tophat function.

- Note: Faraday depth is ***not*** the same as physical depth! (Hence "2.5D") Nor is it like optical depth.

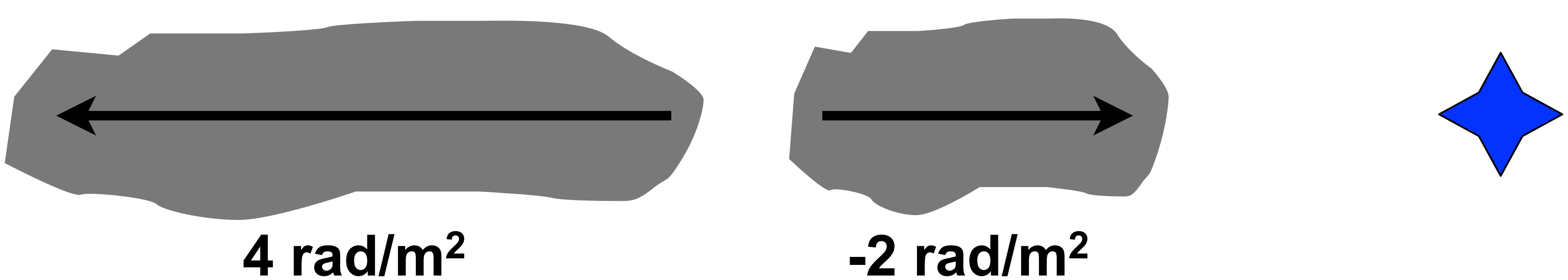

RM Synthesis: In theory

- The equation

$$P(\lambda^2) = \int_{-\infty}^{+\infty} F(\phi) e^{2i\phi\lambda^2} d\phi$$

  is like a Fourier transform, and can (in principle) be inverted to determine the physical situation from the observables.

- However there are some complications:
  - We do not measure $\lambda^2 < 0$
  - We do not measure all $\lambda^2 > 0$

RM Synthesis: In practice

- This leads to a sampling (window) function, and to a finite point spread function (called the ***Rotation Measure Spread Function, or RMSF***). Examples are shown in following slides.
- The formal expression

$$P(\lambda^2) = \int_{-\infty}^{+\infty} F(\phi) e^{2i\phi\lambda^2} d\phi$$

becomes

$$\tilde{P}(\lambda^2) = W(\lambda^2) \int_{-\infty}^{+\infty} F(\phi) e^{2i\phi\lambda^2} d\phi$$

This can be inverted (note the addition of λ_0^2):

$$\tilde{F}(\phi) = K \int_{-\infty}^{+\infty} \tilde{P}(\lambda^2) e^{-2i\phi(\lambda^2 - \lambda_0^2)} d\lambda^2 = F(\phi) * R(\phi) \neq F(\phi)$$

RM Synthesis: In practice

- The expression for the (reconstructed) Faraday dispersion function

$$\tilde{F}(\phi) = K \int_{-\infty}^{+\infty} \tilde{P}(\lambda^2) e^{-2i\phi(\lambda^2-\lambda_0^2)} d\lambda^2$$

can be written as a sum (if channel width is small),

$$\boxed{\tilde{F}(\phi) = K \sum_{c=1}^{N} \tilde{P}_c e^{-2i\phi(\lambda_c^2-\lambda_0^2)}}$$

("trial RM" interpretation)

- The RMSF is then

$$\boxed{R(\phi) = K \sum_{c=1}^{N} w_c e^{-2i\phi(\lambda_c^2-\lambda_0^2)}}$$

$$K = \left(\sum_{c=1}^{N} w_c \right)^{-1}$$

- This operation can be done for a whole field of view (producing an ***RM-cube***).

RM Synthesis: In practice

- RM synthesis works on observed Q,U cubes to produce ***RM-cubes***:

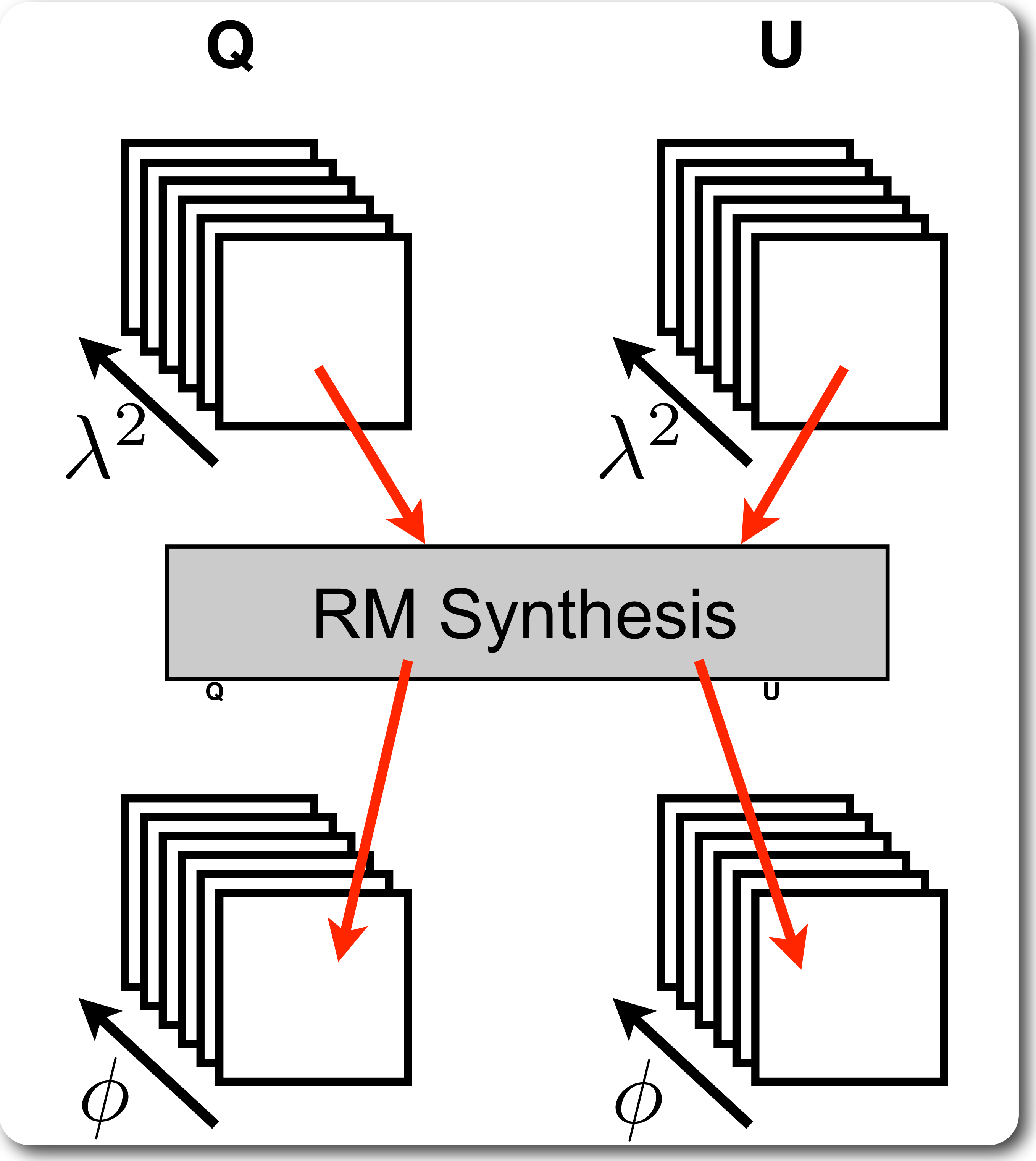

RM Spread Function (RMSF)

$$R(\phi) = K \sum_{c=1}^{N} w_c e^{-2i\phi(\lambda_c^2 - \lambda_0^2)}$$

- Example, two observing bands: 18cm + 21cm λ^2 = .0355, .0455 m^2
- If observed dχ = π
- n π ambiguity becomes π/.01= 314 rad/m^2
- Fringes in RMSF are exactly spaced by this amount.
- If RM synthesis gives same as traditional method, why bother?

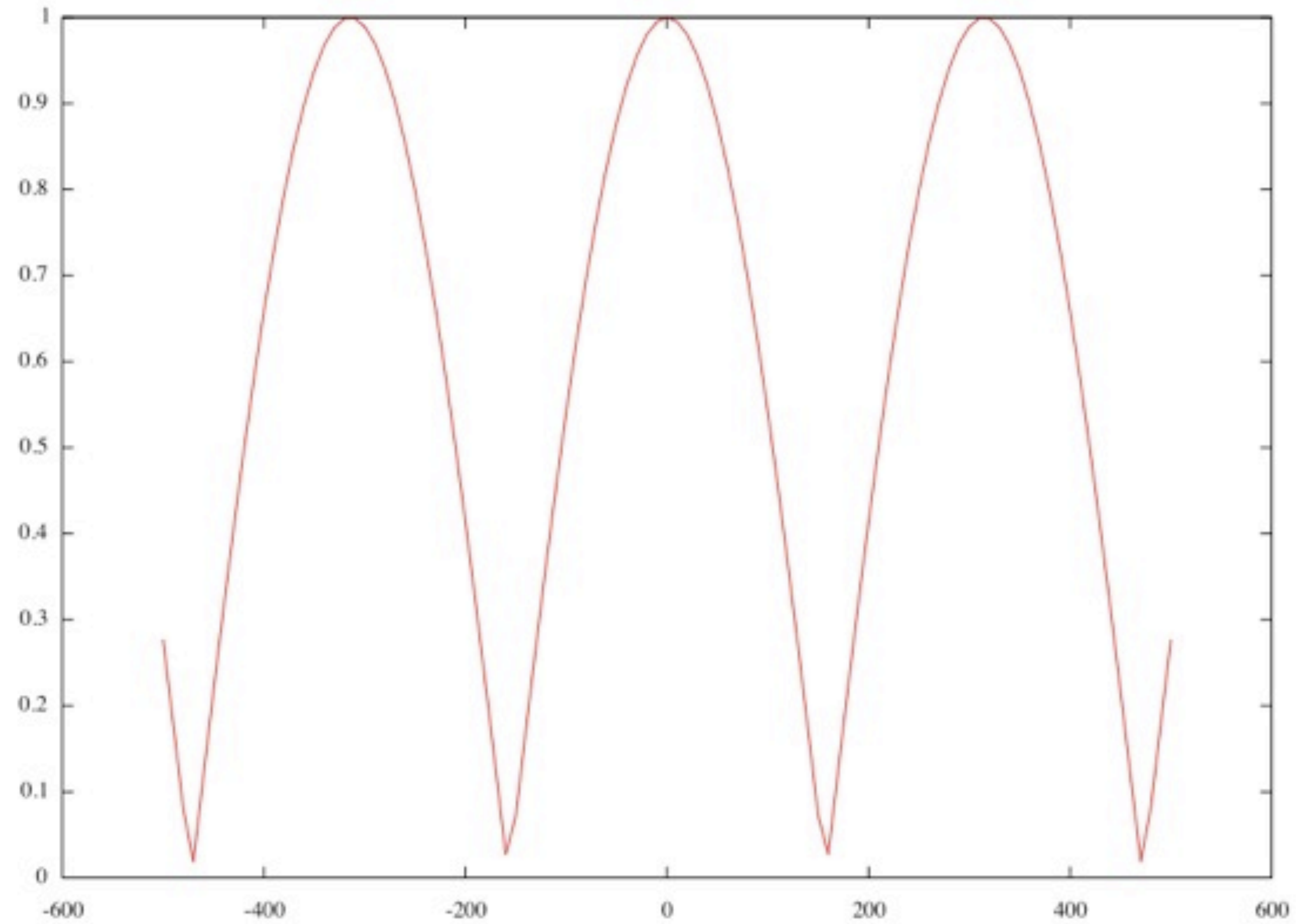

- As with visibilities, do ***not*** need to detect sources in every channel. The transform maximizes S/N.

RM Spread Function (RMSF)

- Example, two observing bands: 18cm + 22cm with 512 channels per band

  real (Q)
  imaginary (U)
  absolute value (P)

$$R(\phi) = K \sum_{c=1}^{N} w_c e^{-2i\phi(\lambda_c^2 - \lambda_0^2)}$$

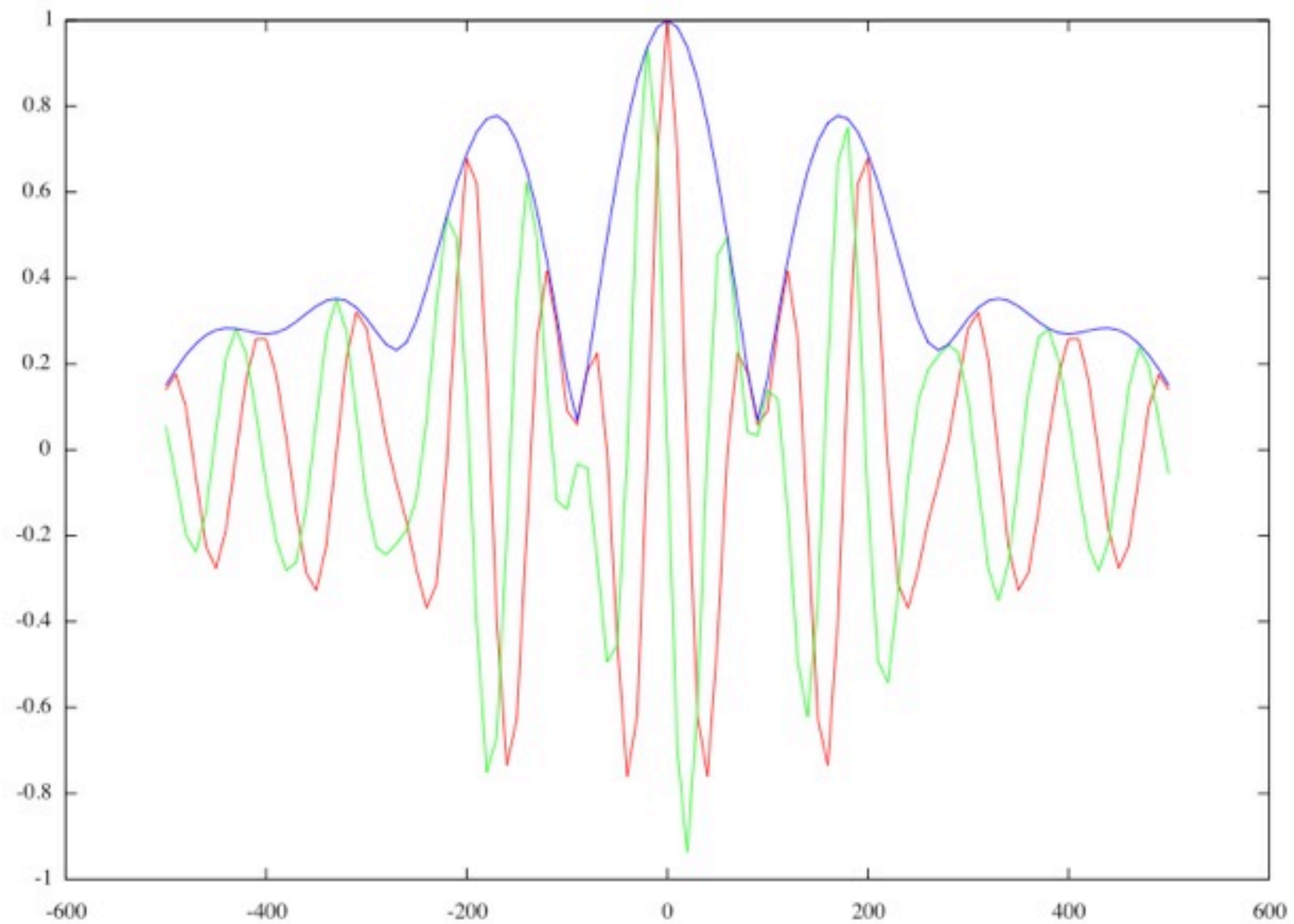

- One can show that the optimal value of λ_0^2 is the weighted mean of the sampled λ^2 values (Brentjens & de Bruyn 2005)

How well can RM be determined?

- From Brentjens & de Bruyn (2005):

$$\sigma_\phi^2 = \frac{\sigma^2}{4(N-2)||P||^2\sigma_{\lambda^2}^2}$$

- Precision in RM determination is achieved by
  - low noise per channel
  - many channels
  - broad frequency (actually, wavelength squared) coverage

Observational design issues

- The performance of RM synthesis is ***strongly*** dependent on the frequency coverage of the observations.
- Key characteristics:
  - Width of RMSF: sensitivity to weak magnetic fields: $\propto \Delta\lambda^2$ (full coverage)
  - Sensitivity to extended Faraday structures (e.g. Burn slabs): $\propto 1/(\min \lambda^2)$
  - Maximum rotation measure before bandwidth depolarization: $\propto 1/\delta\lambda^2$
  - Sidelobe level: "smoothness" of λ^2 coverage (avoid gaps!!)

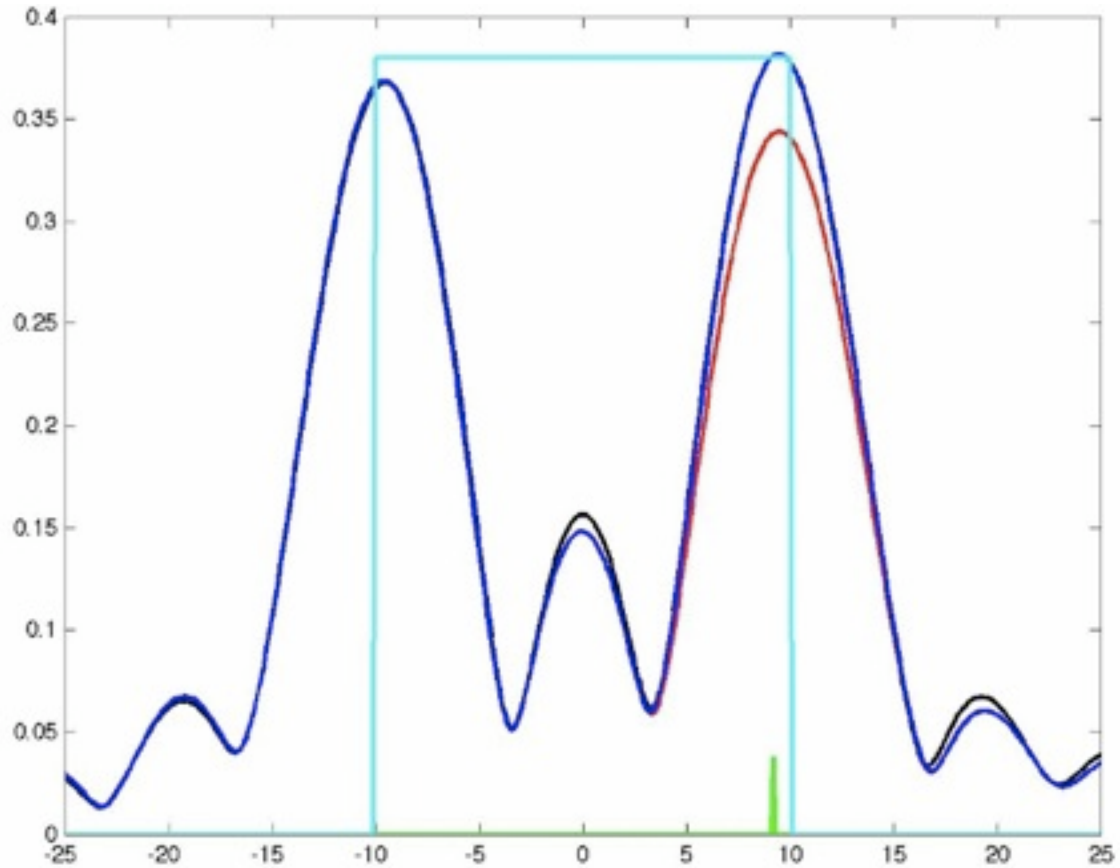

RMSF Deconvolution

- Because of the RMSF, the recovered FDF **must** be deconvolved in situations where multiple components are present

- Technique:
  - Find the peak in the reconstructed Faraday dispersion function
  - Subtract a scaled version of the RMSF, centered at that location
  - Store a delta-function component at that location
  - Iterate until noise floor is reached
  - Convolve delta-function model with restoring RMSF, and add residuals

- 2 broad (160 MHz) bands at 18cm and 22cm (high Faraday depth regime)
- Typical noise levels ~10 μJy/beam rms (6h/galaxy/band)

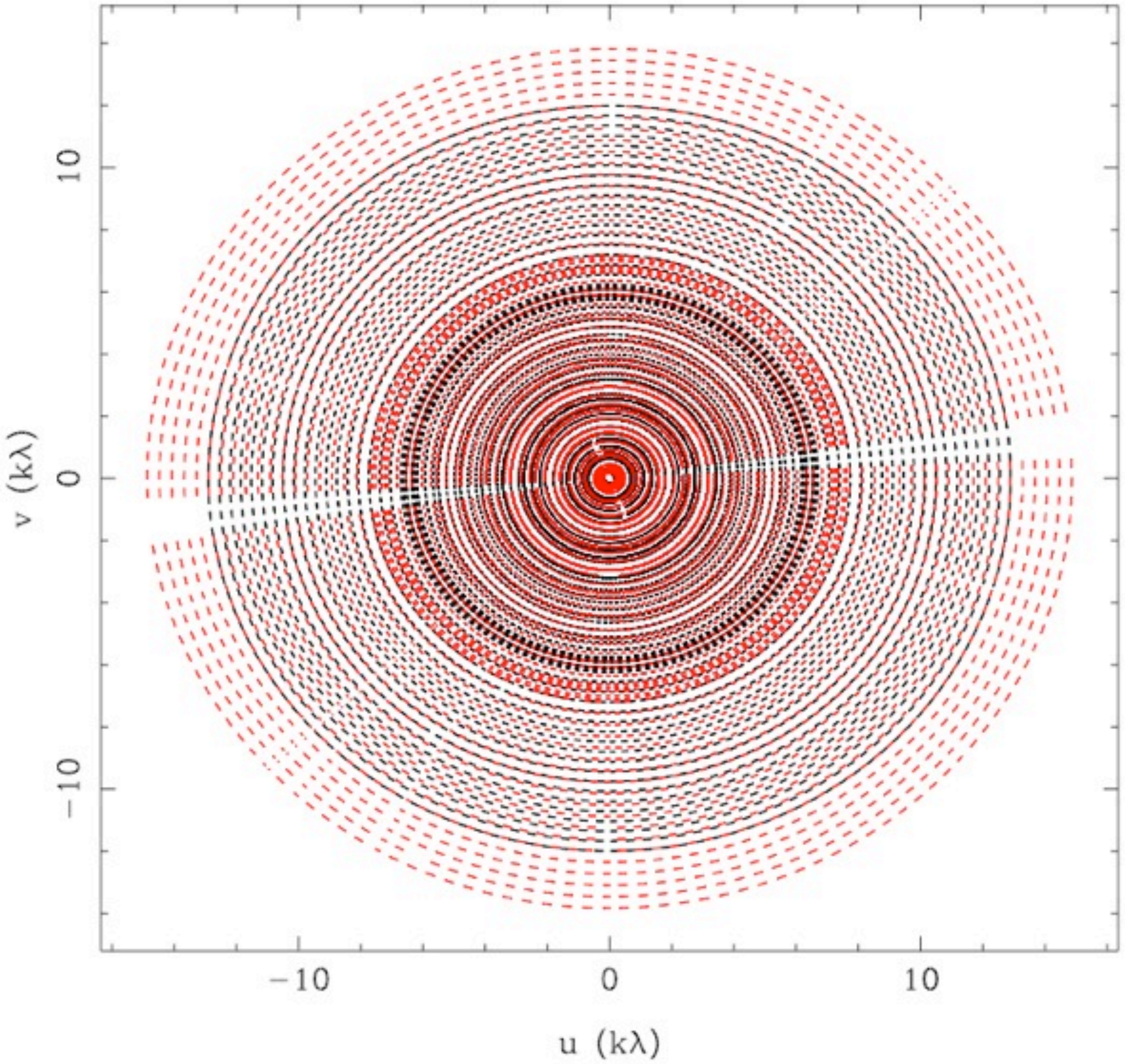

WSRT data analysis

- Data analysed using Rotation Measure Synthesis (RM Synthesis) (see Brentjens & de Bruyn 2005)
  - Fourier transform of observed Stokes (Q,U) over wavelength-squared; provides complex polarization vector as a function of Faraday depth
  - Avoids $n\pi$ ambiguity problems (given sufficient frequency sampling)
  - Coherently adds across the full band, optimizing sensitivity regardless of rotation measure value
- RMSF FWHM ~ 144 rad/m^2
- Faraday dispersion functions deconvolved using RM-CLEAN (see Heald et al. 2009; code available online)
- Polarized flux and rotation measure values extracted using moment-map techniques standard in the emission line (e.g. HI) community

Results

- 28 galaxies studied
  21 detected in polarization
  - 0/4 Magellanic/elliptical
  - 21/24 spirals

Optical image courtesy Robert Gendler

Resulting images

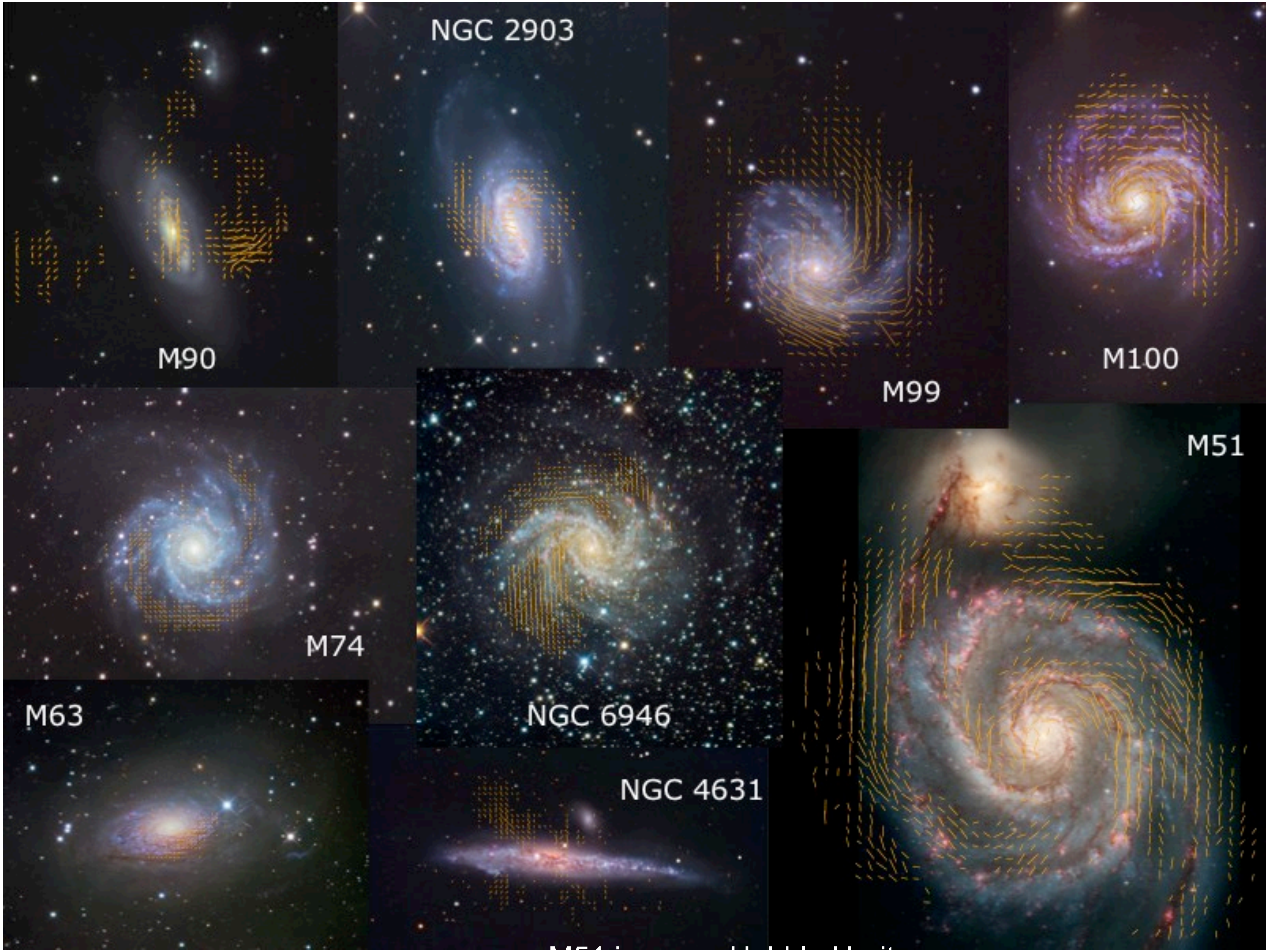

- approaching side
- receding side

PA = 243°

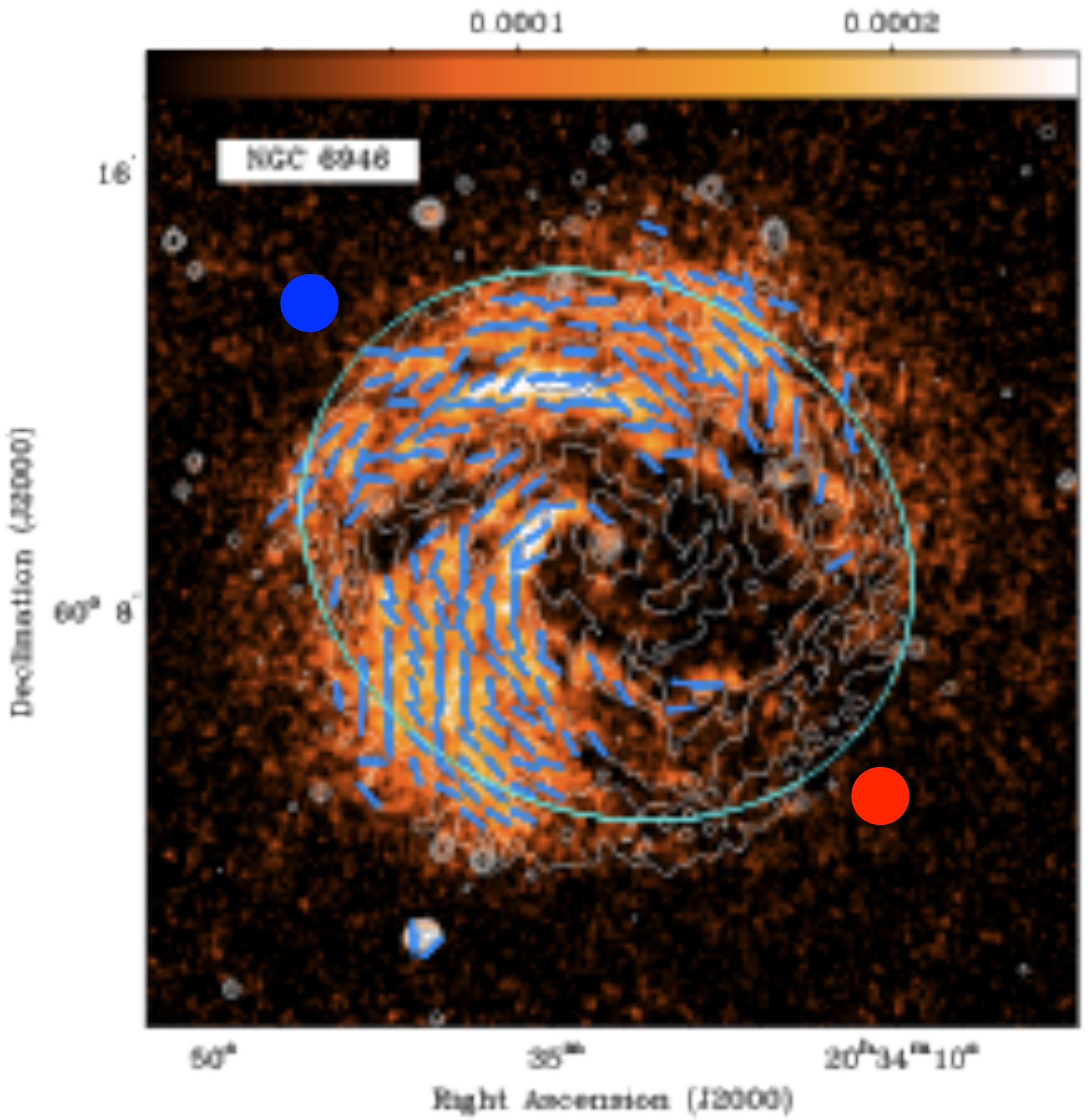

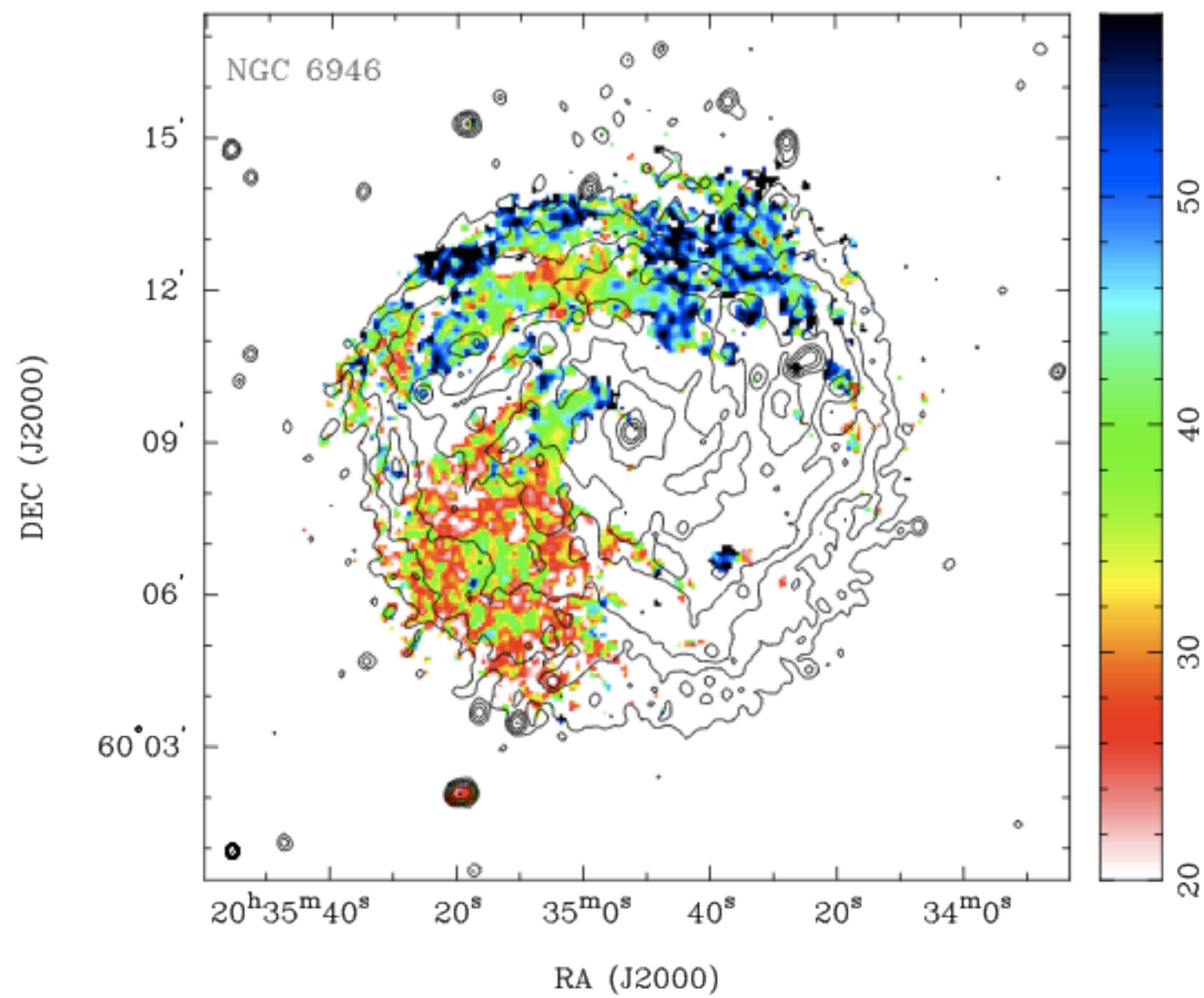

approaching side

receding side

LOFAR ASTRON

PA = 159°

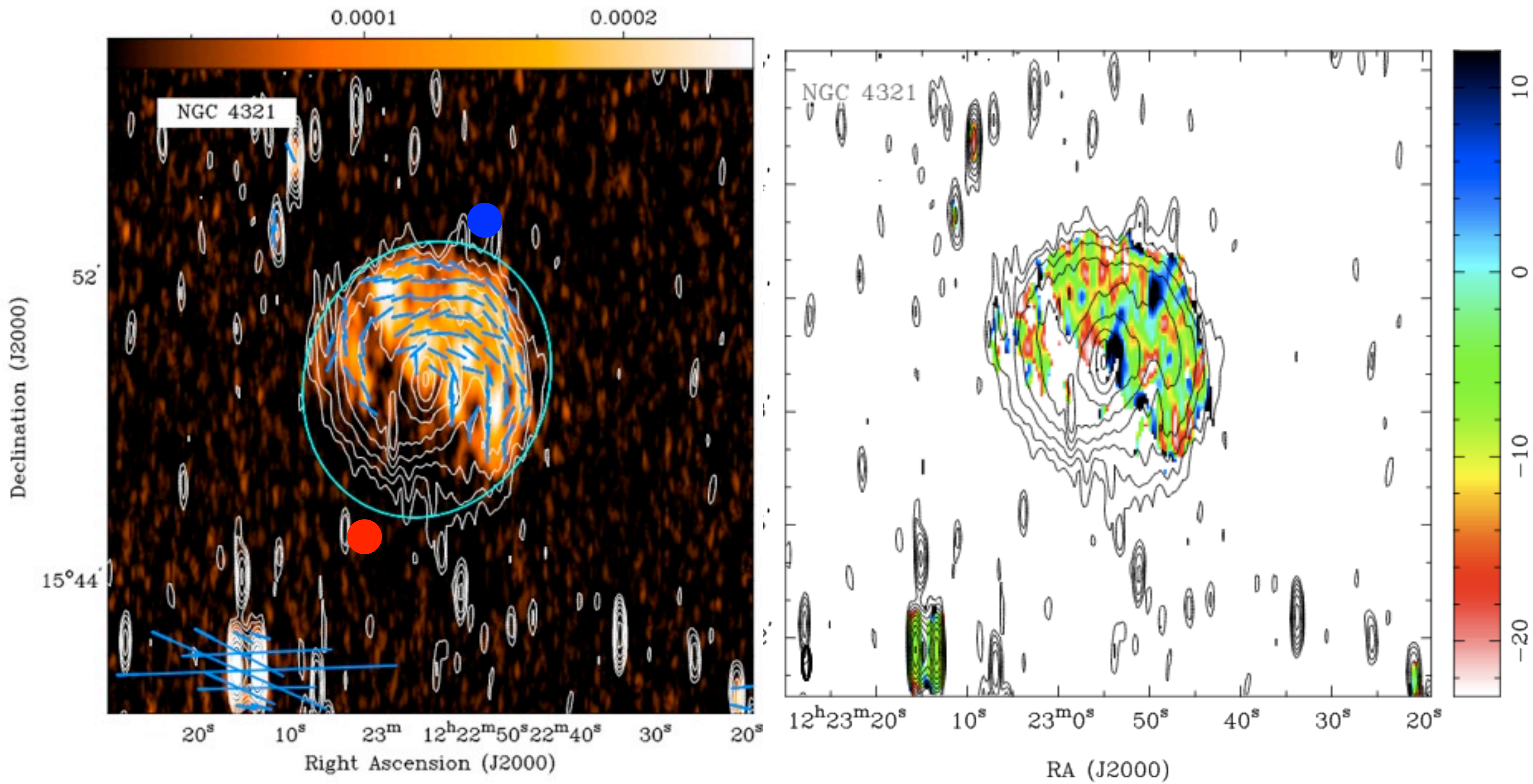

Trend in P(θ)

- Minimum in P consistently found on the receding major axis -- WHY?

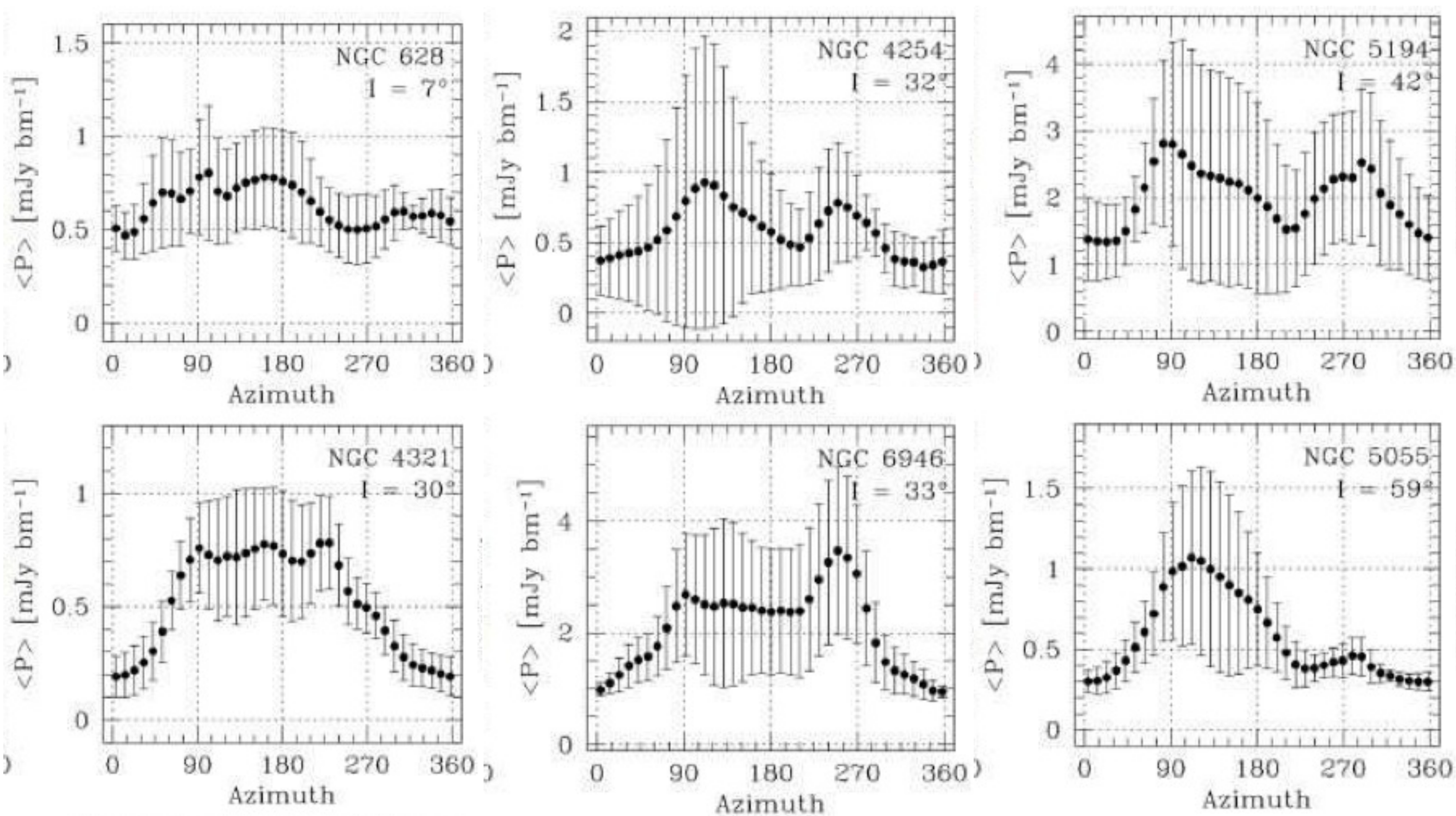

Trend in P(θ)

- Minimum in P consistently found on the receding major axis -- WHY?

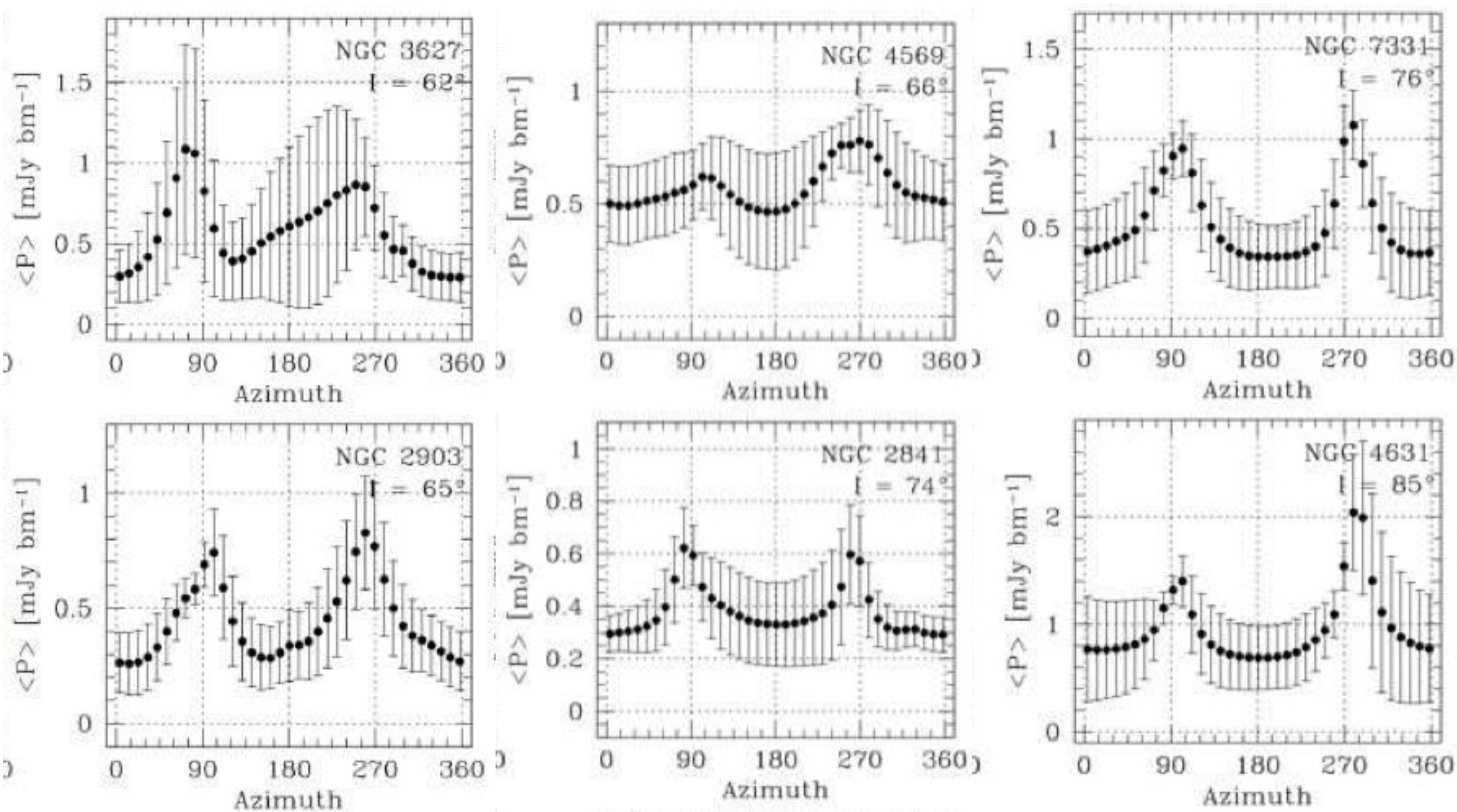

- Combination quadrupolar field + axisymmetric spiral (NB: *geometry only*)

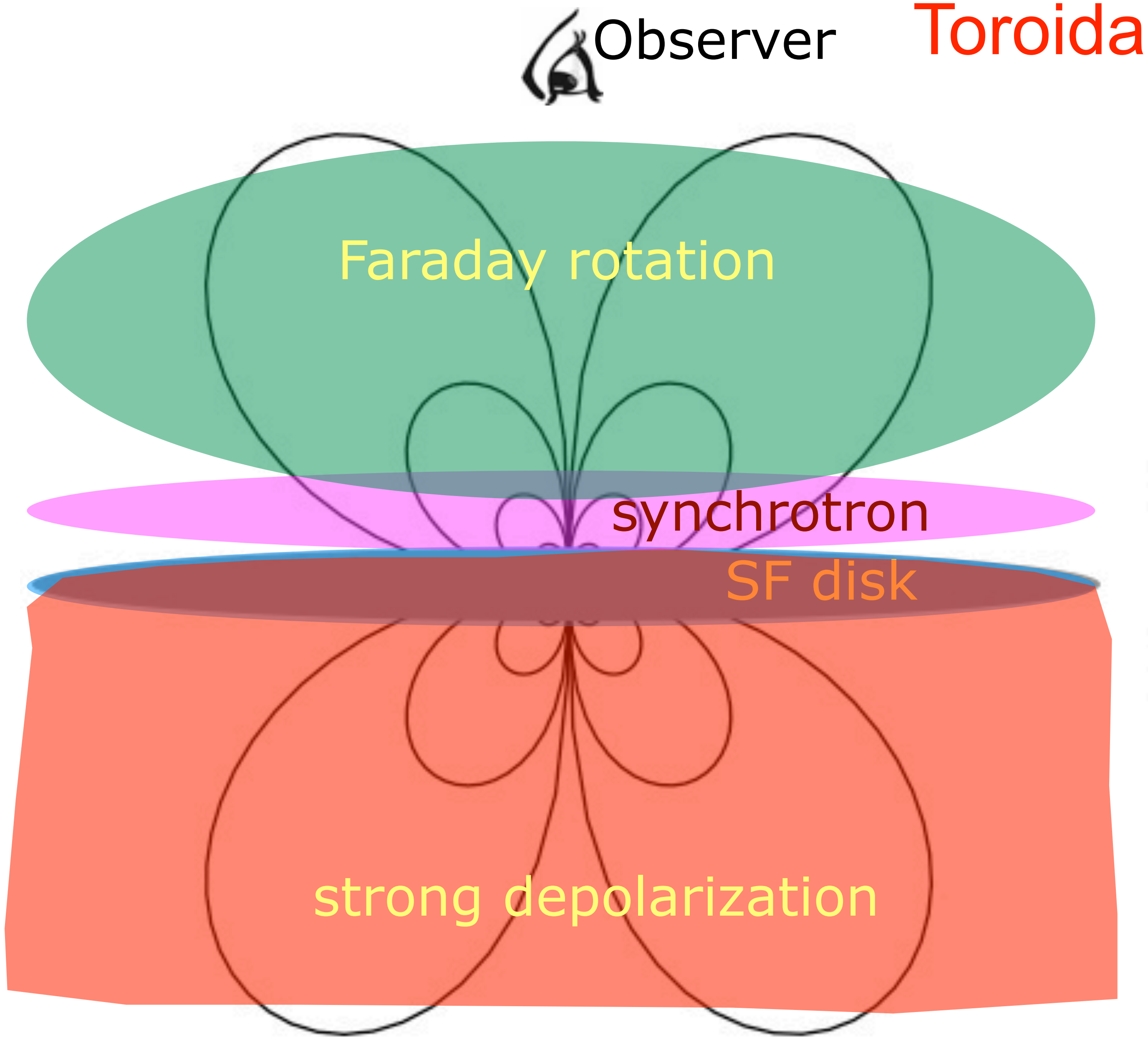

Toroidal & poloidal fields in same sense

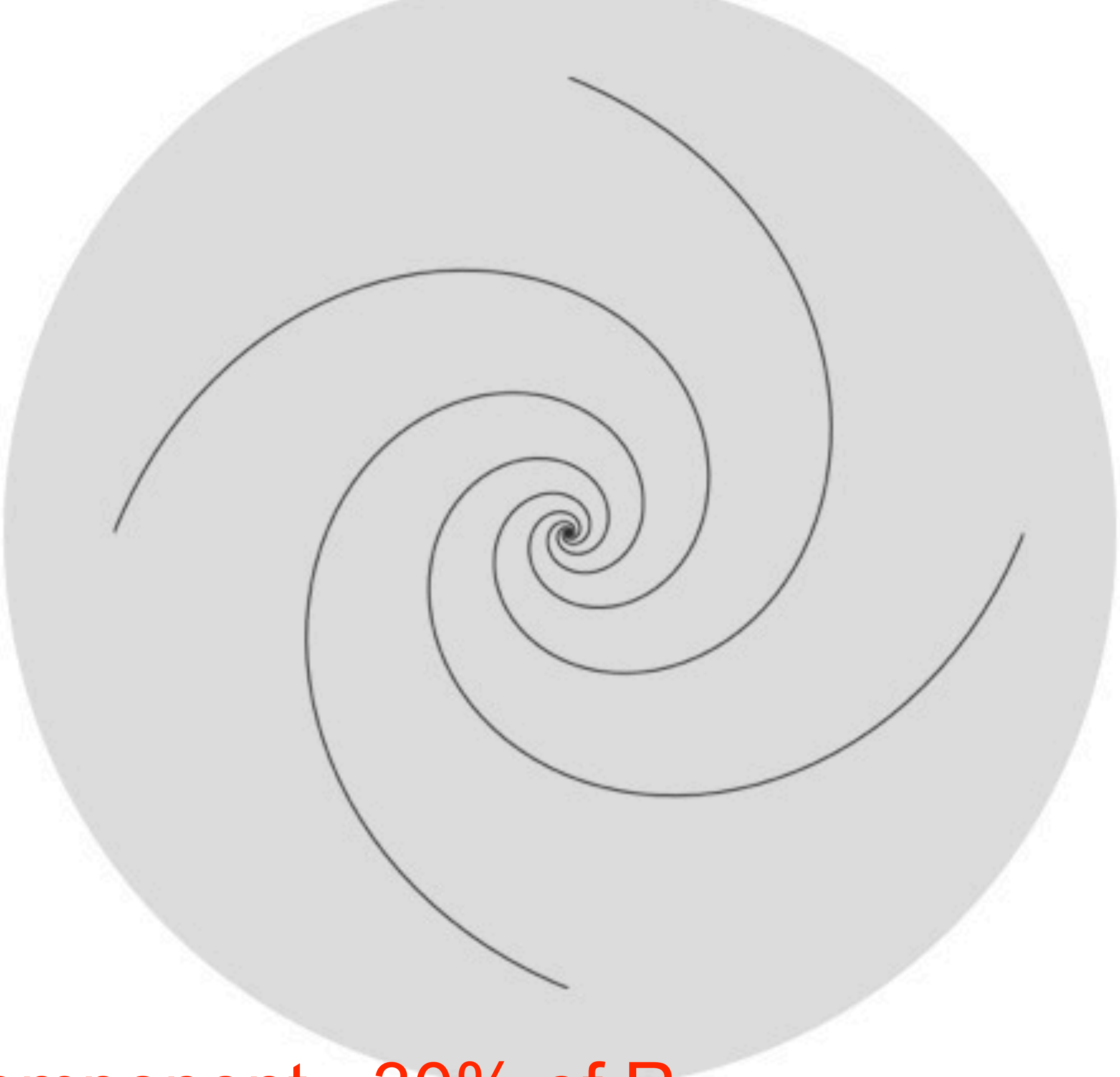

Vertical extent of spiral component ~30% of R

Interpretation

- Azimuthal asymmetry by field projection ("square styrogalaxy model")

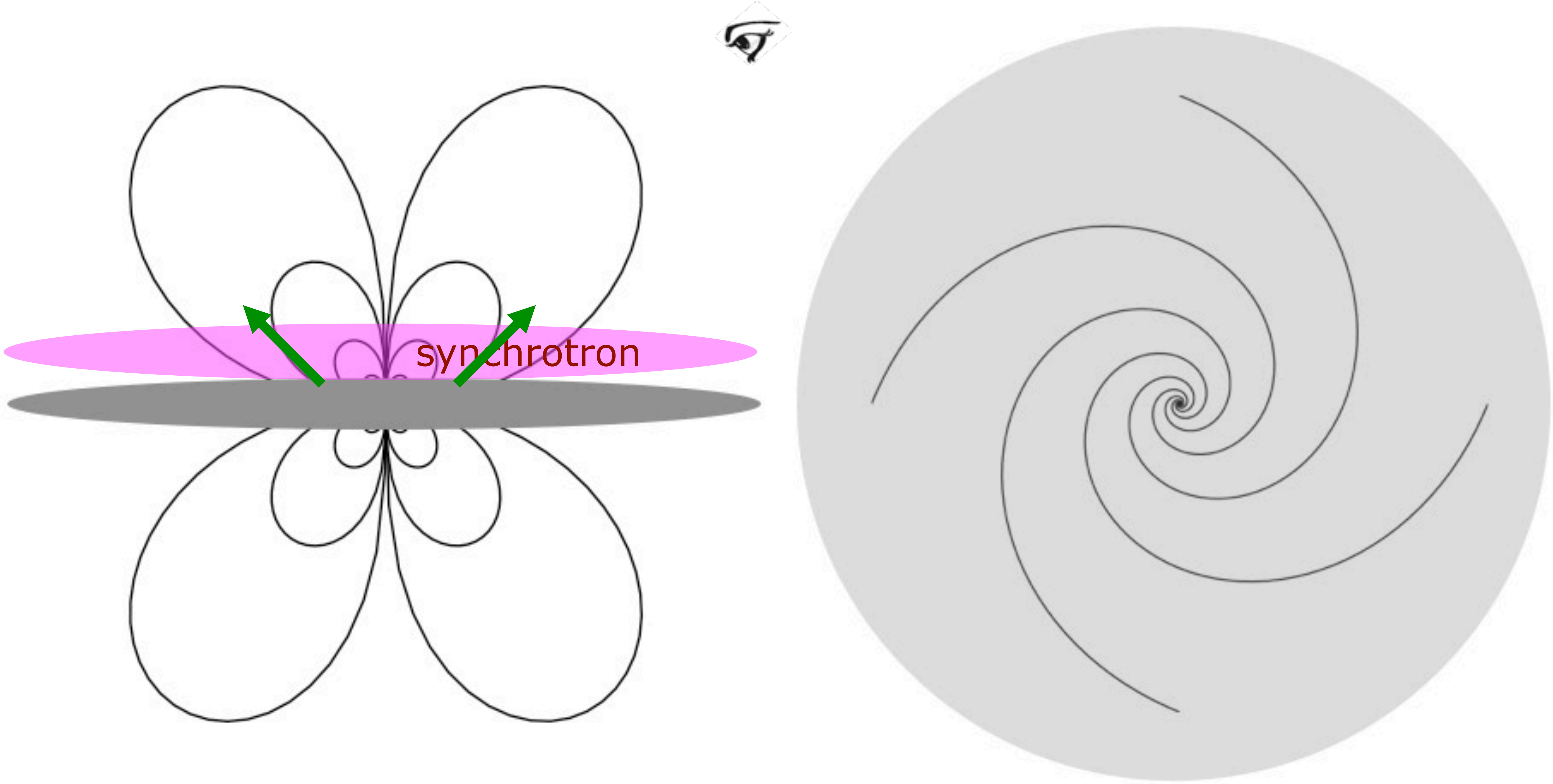

Interpretation

- Such a geometrical model reproduces the correct effect
- (see also Urbanik et al. 1997, who showed a similar model)

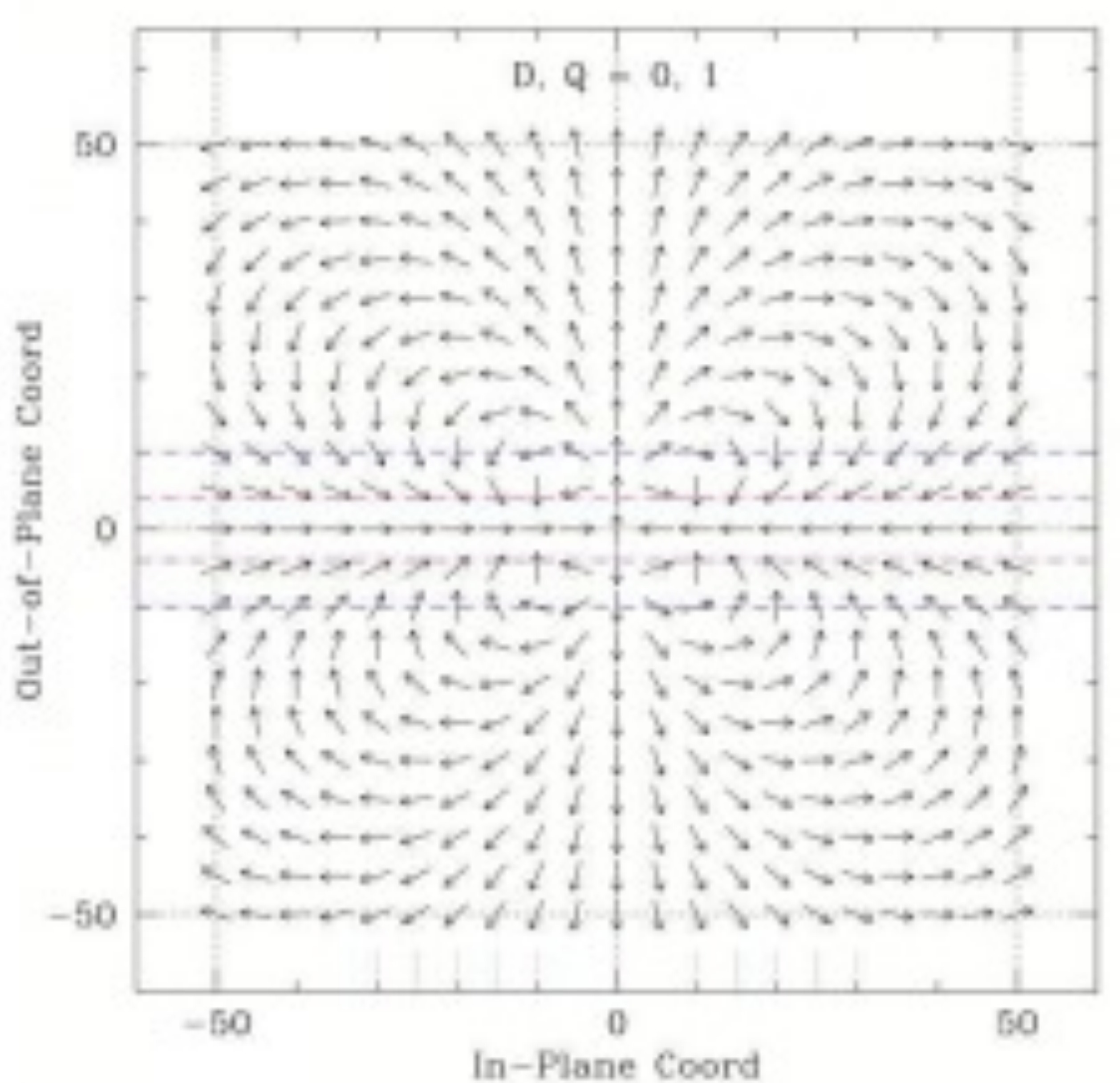

Braun et al. (2010)

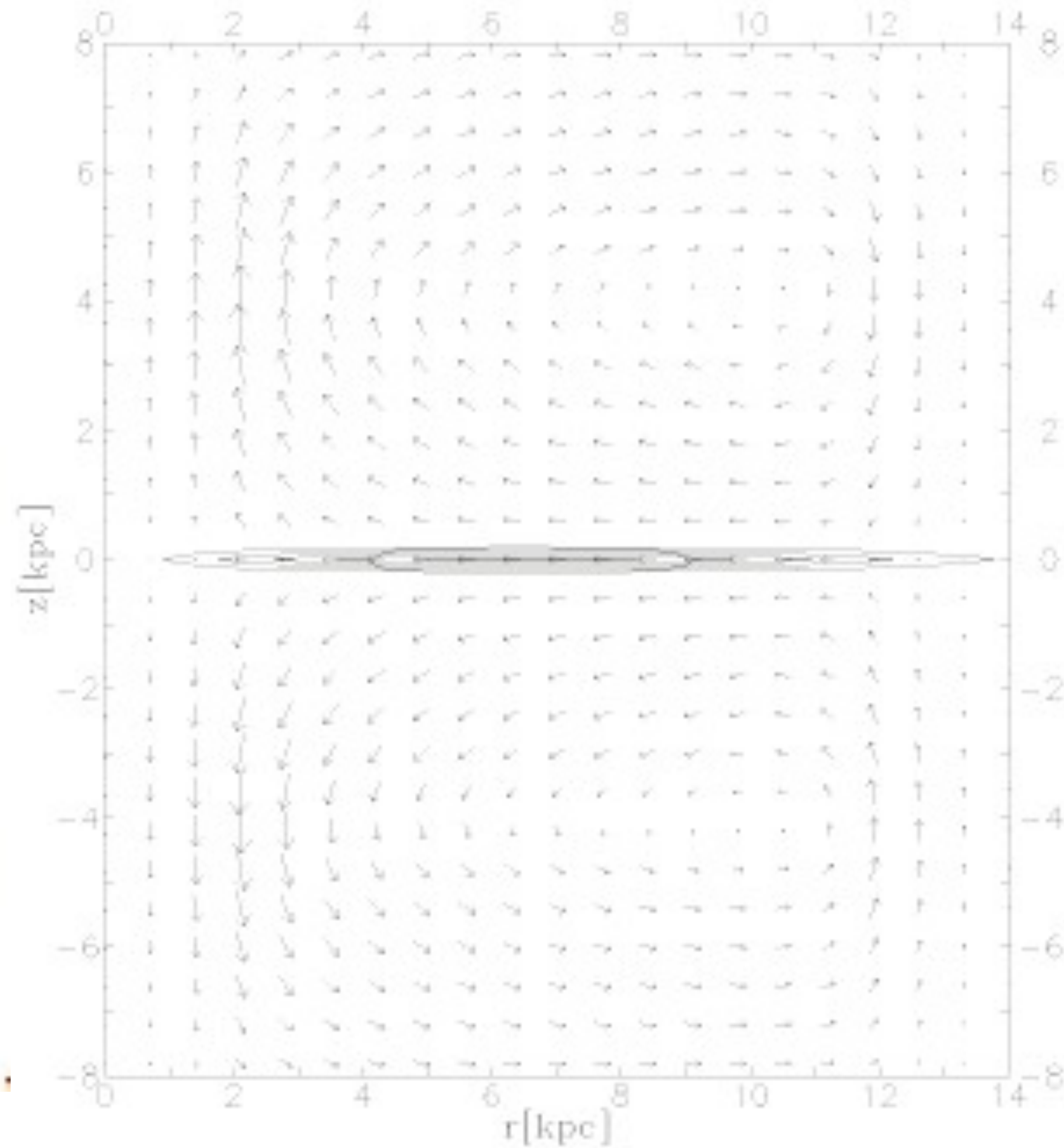

Urbanik et al. (1997)

A faint view of the disk backside

- RM Synthesis reveals polarized emission at extreme values of Faraday depth – possibly originating from behind the depolarizing medium

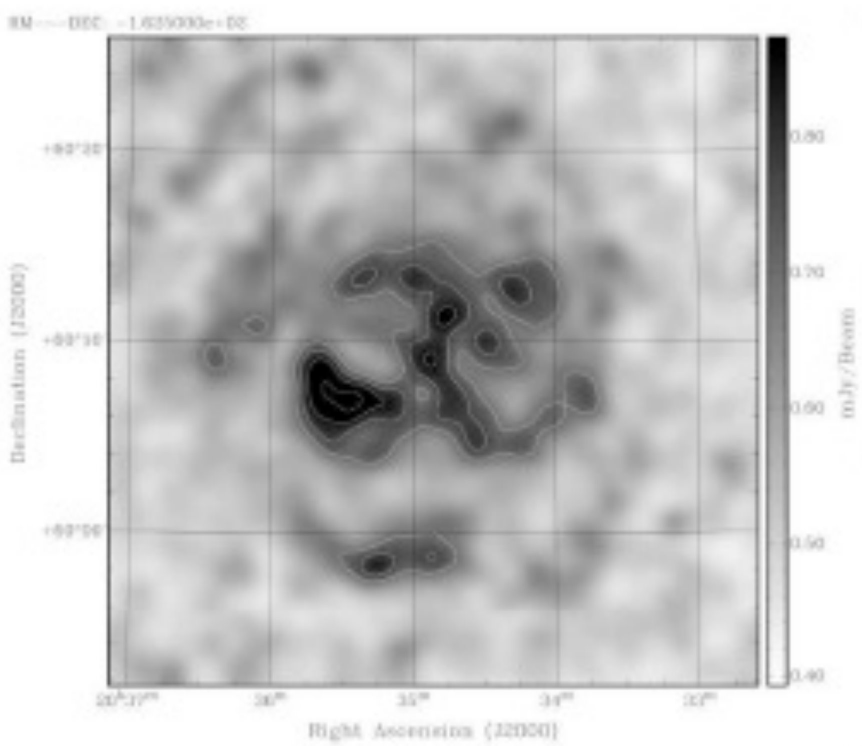

-162 rad/m^2

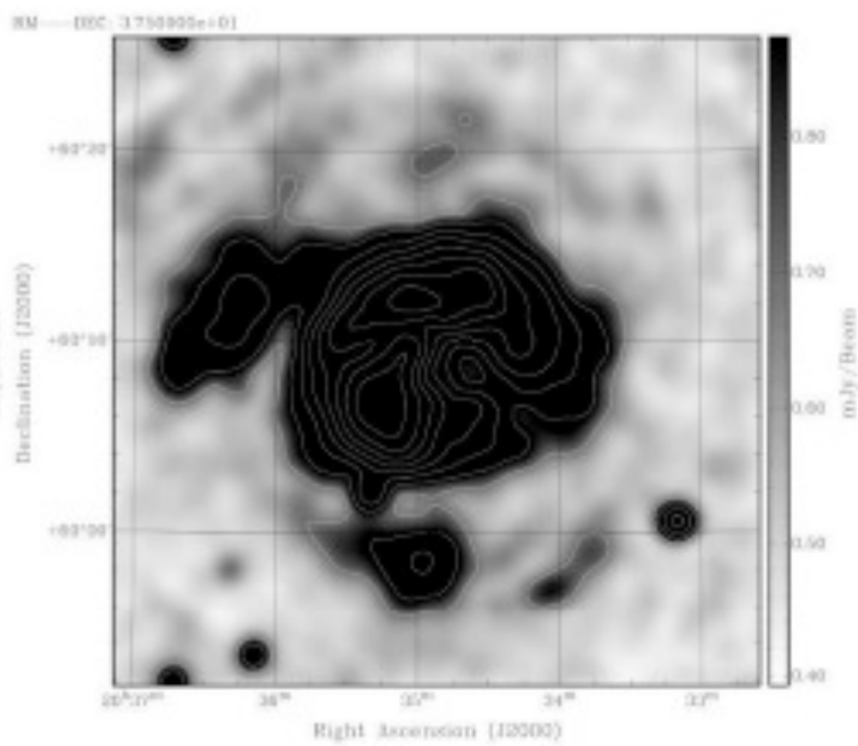

+38 rad/m^2

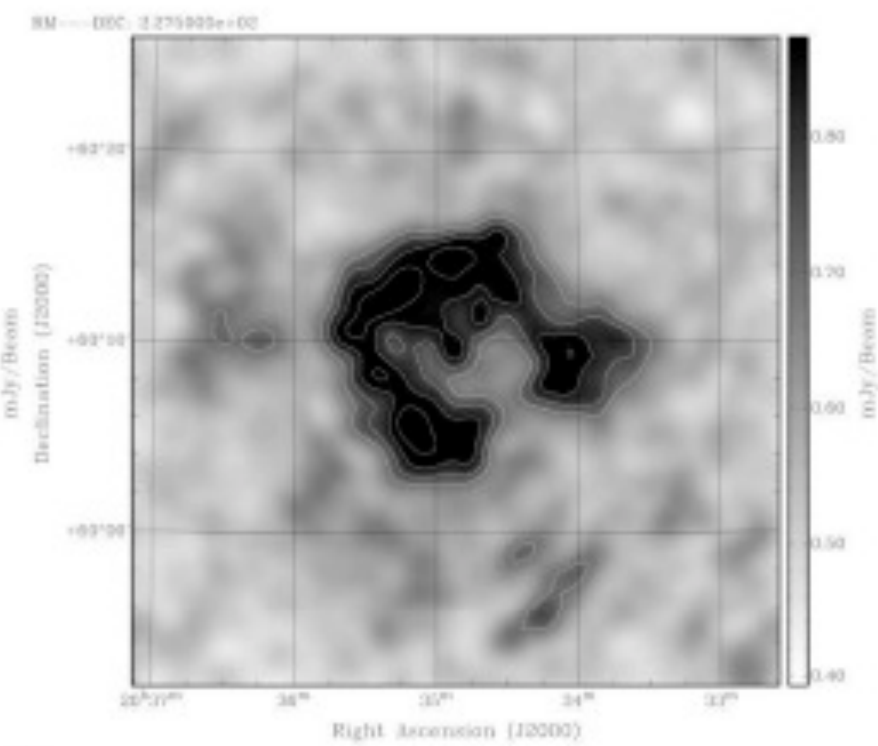

+228 rad/m^2

- Prediction: azimuthal asymmetry vanishes at higher frequency

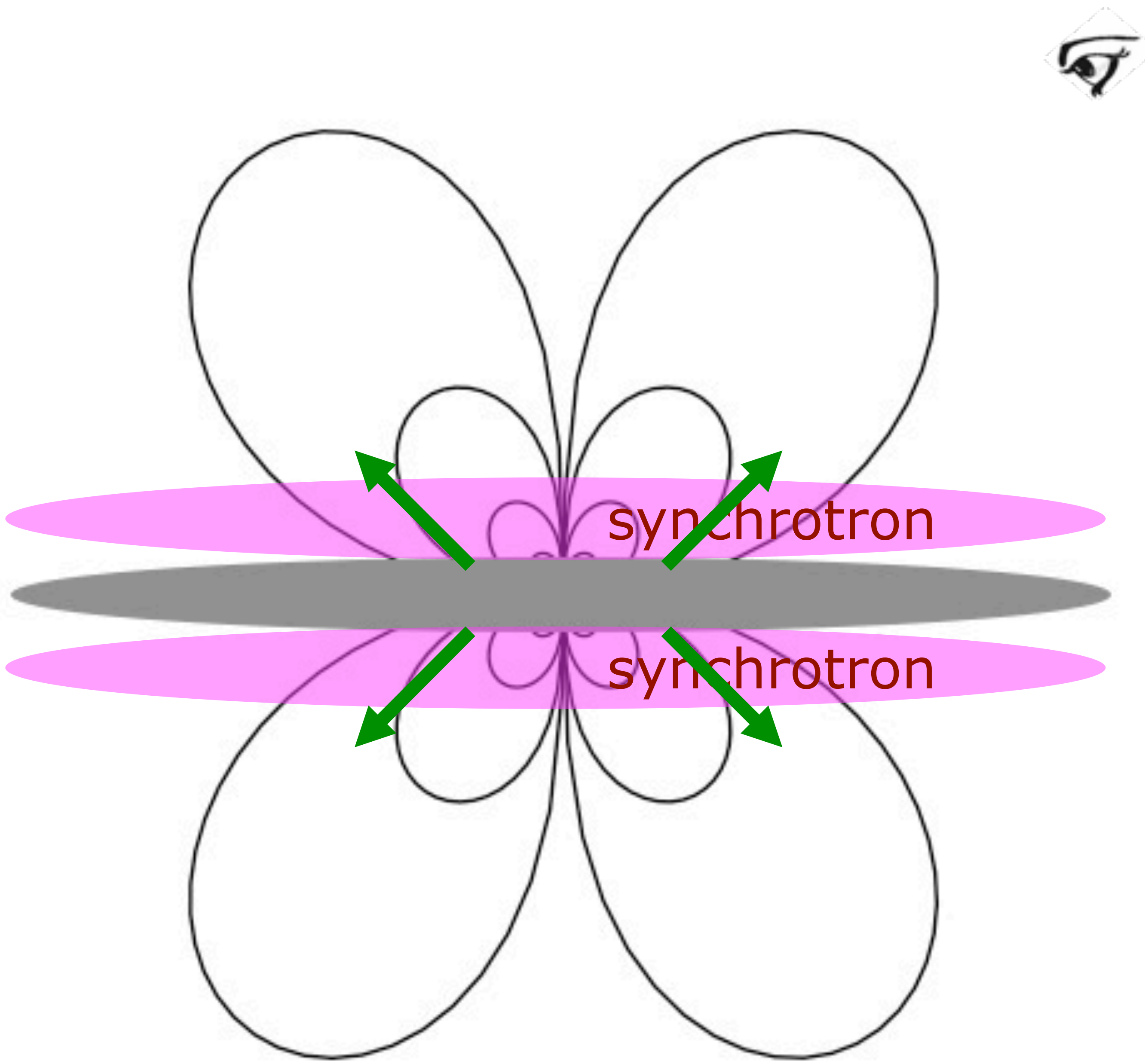

Interpretation

- Prediction: azimuthal asymmetry vanishes at higher frequency
- Seems to be the case in NGC 6946 (Beck)
- True for others? (NGC 4321?)

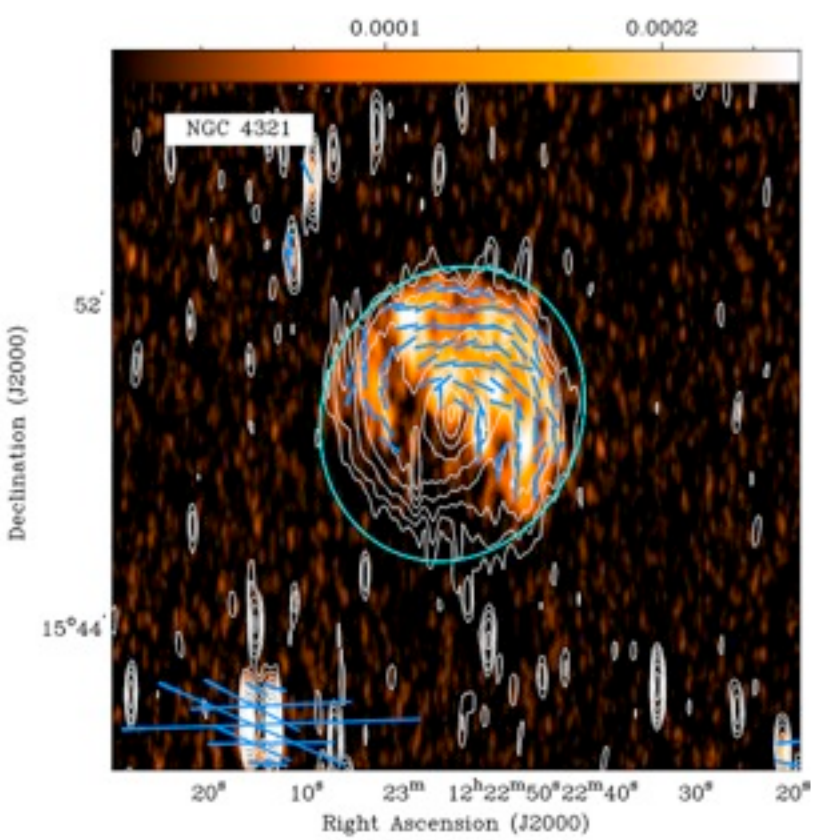

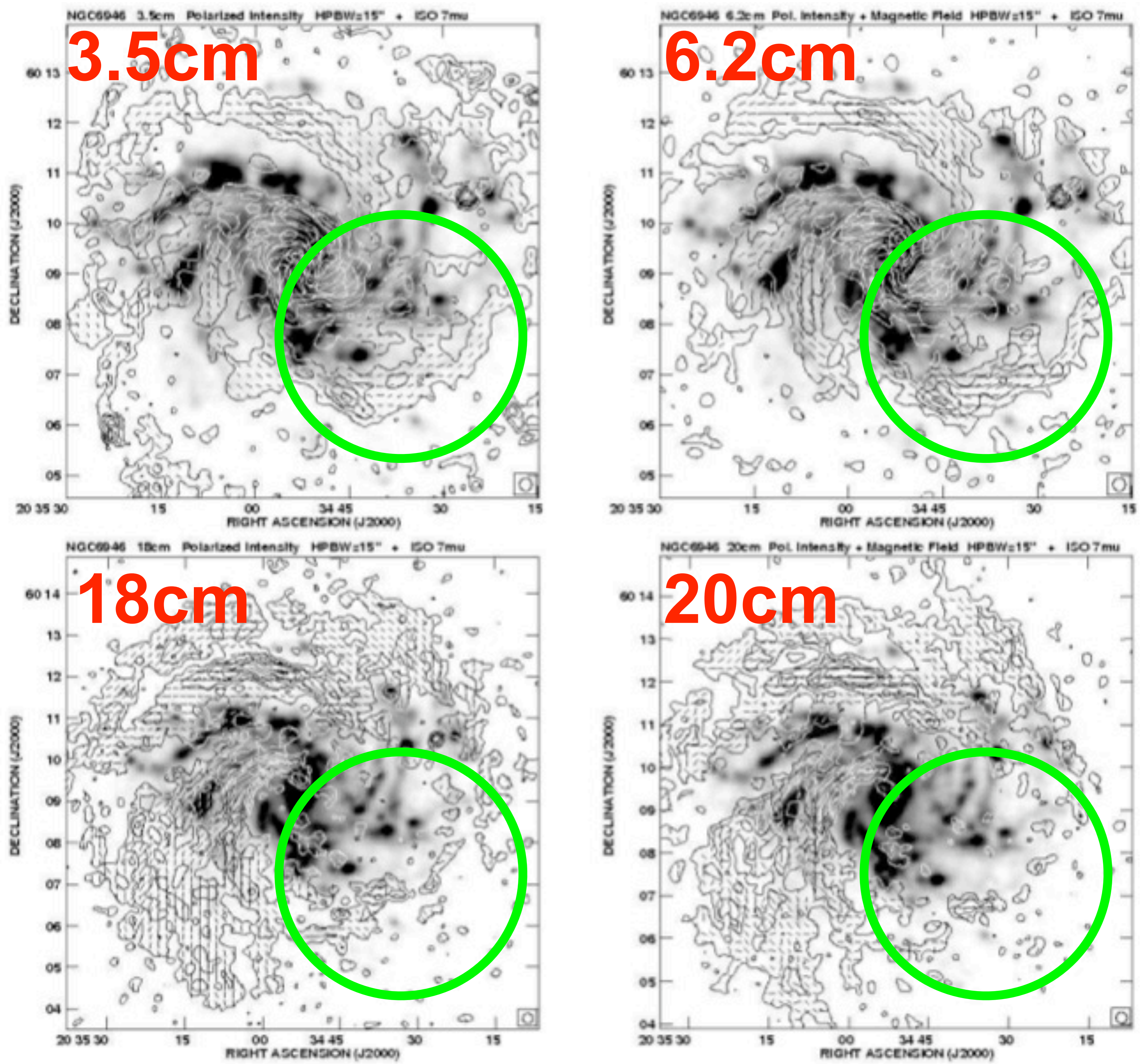

Significance

- A combination of planar and poloidal field such as this is predicted by dynamo theory (e.g. Widrow 2002)
- Dominance of axisymmetric over bisymmetric, and quadrupolar over dipolar, should give strong constraints to dynamo models

Significance

- A combination of planar and poloidal field such as this is predicted by dynamo theory (e.g. Widrow 2002)
- Dominance of axisymmetric over bisymmetric, and quadrupolar over dipolar, should give strong constraints to dynamo models

- Note that our edge-on targets actually show evidence for *dipolar* magnetic fields in the outer halo - again, predicted by dynamo theory. Why the difference? Signature of dipolar outflow?

Aside: rotation of halo gas

- Multiphase gas at large vertical distances above the midplane commonly observed in nearby galaxies
- Rotation of this extraplanar gas reveals a linear decrease in rotation speed with height – halos differentially rotate, but with a slower amplitude than the underlying disk (Fraternali et al. 2005; Heald et al. 2006, 2007)
- Connection between kinematics of gaseous halos and the vertical structure of the halo gas? (see Heald et al. 2007)

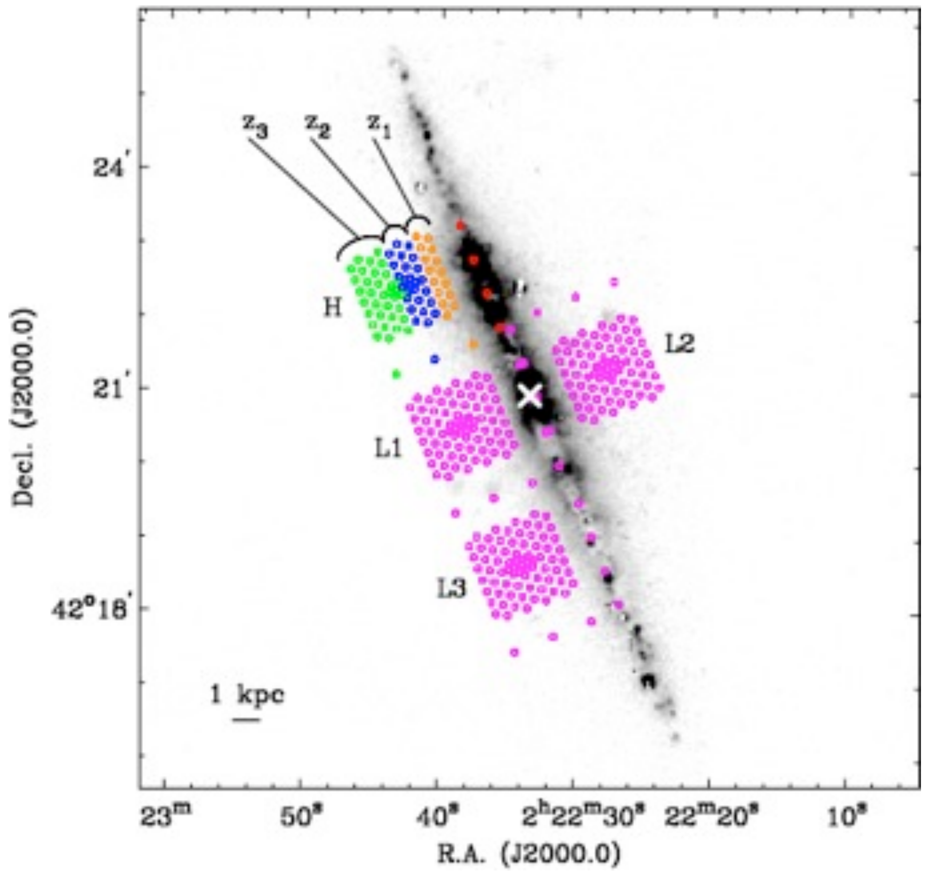

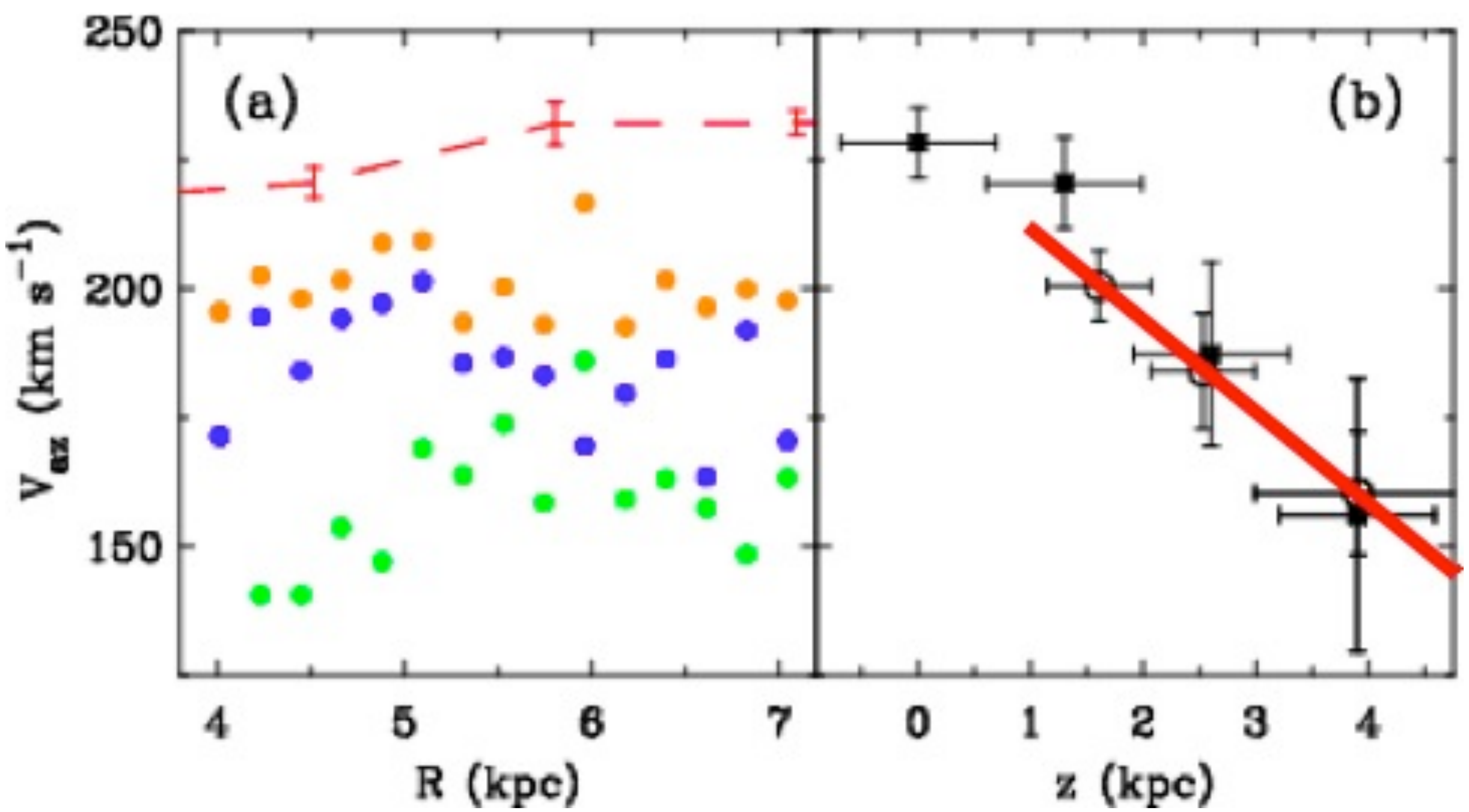

Future work

LOFAR ASTRON

- LOFAR will probe the outer disks and halos of a large number of nearby galaxies, characterizing the global magnetic field geometry
- Do halo fields become predominantly dipolar in the far outer parts?
- How far do the halo fields extend?

- Complementarity between LOFAR, and other higher-frequency instruments (APERTIF, ASKAP, MeerKAT, EVLA, ...)
  - each probes a different 'zone' of the galaxy
  - gives an onion-peel view of galactic magnetic field structure!

Future work

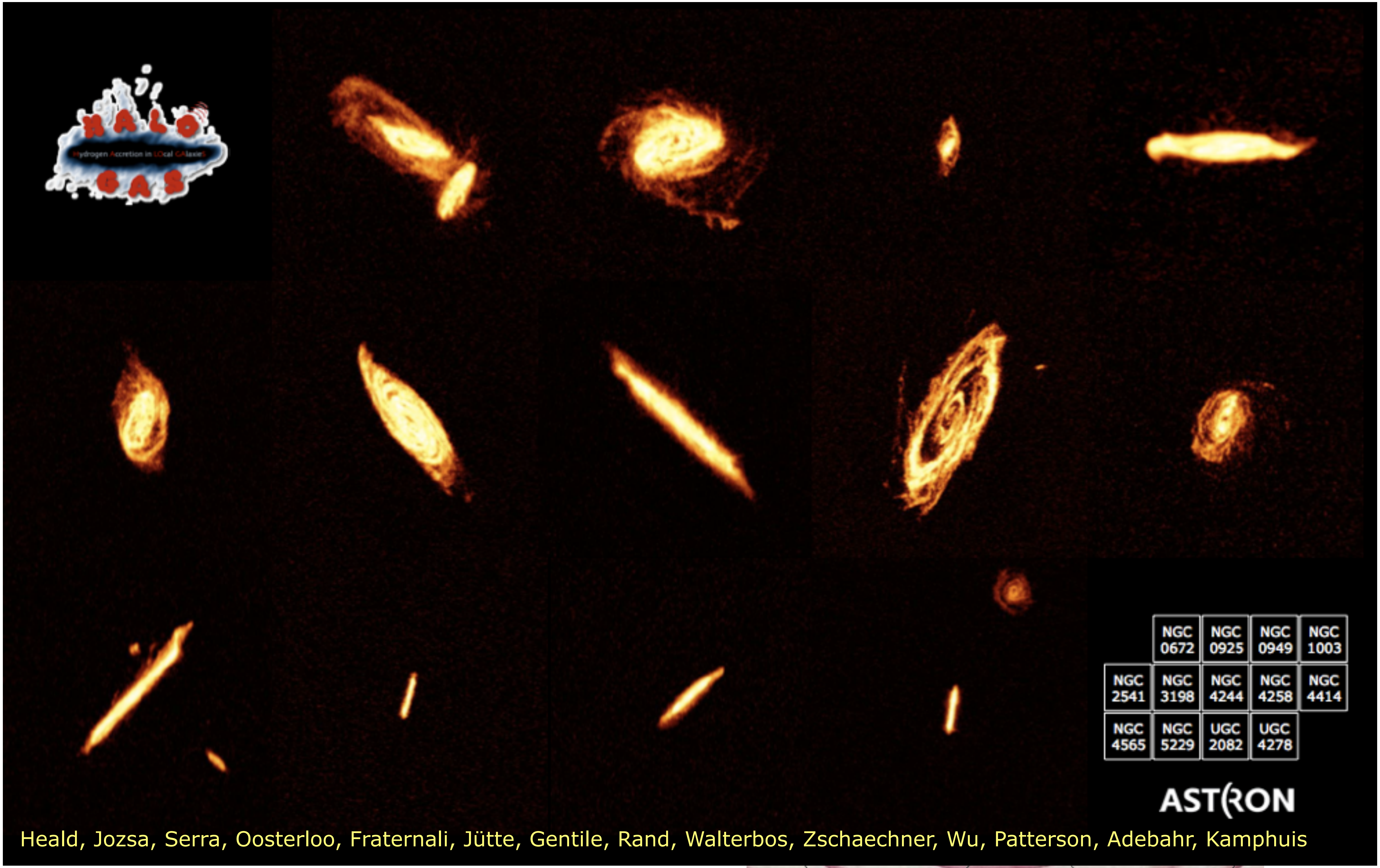
HALO GAS
Hydrogen Accretion in LOcal GAlaxieS
NGC 0672
NGC 0925
NGC 0949
NGC 1003
NGC 2541
NGC 3198
NGC 4244
NGC 4258
NGC 4414
NGC 4565
NGC 5229
UGC 2082
UGC 4278
ASTRON
Heald, Jozsa, Serra, Oosterloo, Fraternali, Jütte, Gentile, Rand, Walterbos, Zschaechner, Wu, Patterson, Adebahr, Kamphuis

LOFAR today

- LOFAR station status visible online at
  http://www.astron.nl/~heald/lofarStatusMap.html
- Interferometry mode works well (fringes and images on 600-km baselines @ 30 MHz!); Imaging pipeline in good shape (Heald+ arXiv:1008.4693)

Summary

- Asymmetry in polarized intensity in nearby galaxies caused by combination of toroidal and poloidal components
  - Minimum P/I on receding side: consequence of *trailing spiral arms*
  - Asymmetry expected to vanish at higher frequency

- New observational programs with LOFAR and other (higher frequency) new telescopes will allow us to learn much more about the full 3-D structure of galactic magnetic fields